

A Novel Methodology for Epidemic Risk Assessment: the case of COVID-19 outbreak in Italy

A. Pluchino¹, G. Inturri², A. Rapisarda^{1,3}, A. E. Biondo⁴, R. Le Moli⁵,
C. Zappalà¹, N. Giuffrida⁶, G. Russo⁷, V. Latora^{1,3,8,9}

Abstract

We present a novel methodology in order to perform the epidemic risk assessment in terms of different factors which are useful to understand the different impact of an epidemic in different areas of a country. In particular we discuss the case of COVID-19 outbreak in Italy. We characterize each region of Italy by considering the available data on air pollution, mobility, winter temperature, housing concentration, health care density, total and aged population. We find that the epidemic risk is higher in some of the northern regions of Italy with respect to central and southern part. Our epidemic risk index shows strong correlations with the available official data of the COVID-19 outbreak in Italy and explain in particular why regions like Lombardia, Emilia-Romagna, Piemonte and Veneto are suffering much more than the rest of the country in terms of infected cases, intensive care units and deceased patients. Although the COVID-19 outbreak started almost in the same period, at the beginning of 2020, in both north (Lombardia and Veneto) and central part of Italy (Lazio), when the first infected were officially certified, the outbreak has been more diffuse and lethal only in those regions with higher epidemic risk. Due to the fact that a large part of infected people do not show evident symptoms of the disease, we claim that in the regions with a lower epidemic risk, i.e. the central and south part of Italy, the epidemic, although probably already very diffused, should not be as lethal as in the northern part of Italy due to a different *a-priori* risk exposure. We also discuss some policy implications directly connected with our methodology, which results to be very flexible and adaptable to different set of epidemic historical data and to different countries.

Keywords: Epidemic risk assessment, COVID-19 outbreak, Italy, Air Pollution, Air Mobility, Strategies for outbreak containment.

¹ Dipartimento di Fisica e Astronomia “Ettore Majorana”, Università di Catania and INFN Sezione di Catania, Italy;

² Dipartimento di Ingegneria Elettrica Elettronica e Informatica, Università di Catania, Italy;

³ Complexity Science Hub Vienna, Austria;

⁴ Dipartimento di Economia e Impresa, Università di Catania, Italy;

⁵ Dipartimento di Medicina Clinica e Sperimentale - UO di Endocrinologia - Ospedale Garibaldi Nesima - Università di Catania, Italy;

⁶ Dipartimento di Ingegneria Civile e Architettura, Università di Catania;

⁷ Dipartimento di Matematica e Informatica, Università di Catania, Italy;

⁸ School of Mathematical Sciences, Queen Mary University of London, London E1 4NS, UK

⁹ The Alan Turing Institute, The British Library, London NW1 2DB, UK

1 Introduction

The prediction of the future developments of a natural phenomenon is one of the main goals of the scientists. Prediction in science is based on the understanding of the key ingredients which characterize the observed natural phenomena. The scientific method that we use since Galileo Galilei, is based on the detailed observation of the phenomenon under study, the formulation of a reasonable theory that is supposed to make new predictions. These are in turn compared with experimental observations. If the theoretical predictions do not agree with the observations, the theory is adjusted or changed to take into account the new experimental evidence. The process is iterated until convergence is reached and discrepancies between theory and experiment are minimized. With the advent of big data, powerful computers and artificial intelligence, many have started thinking that theoretical models are unnecessary, and predictions can be made by direct processing the existing data. In several fields this has proved to be very successful, but prediction without understanding the main causes of a phenomenon is limited and quite dangerous. Very often spurious correlation can emerge and it is difficult to discriminate a true cause from a pure coincidence. In any case, predicting the future remains always a great challenge especially when the phenomenon that one is observing involves people that can have a feedback reaction on the observed quantities which characterize the phenomenon. This is particularly true in the case of epidemics, especially with the COVID-19 outbreak that the world is suffering in this period.

COVID-19 (SARS-CoV-2) is a novel coronavirus initially announced as the causative agents of pneumonia of unknown etiology in Wuhan city, China. The genome sequences is related to a viral species named severe acute respiratory syndrome (SARS) related-CoV. These viral species also comprises some viruses detected in rhinolophid bat in Europe and Asia (Zhang 2019, Peiris 2003). A specific protein (S protein) of virus surface facilitates viral entry in the target cells by angiotensin converting enzyme (ACE2) receptor but the mechanisms of immunological response to the virus infection are incompletely known (Hoffman et al. 2020). The majority of infections by coronavirus are mild and self-treated, therefore, to estimate the spread by hospital and general practitioner reports, can be misleading in the early stages of the disease evolution. This is the reason why the majority of countries are actually counting the reports and not how many people have the virus. Those reports vary according to how the numbers are measured, the number of tests being related to the number of symptomatic patients.

For all these reasons, even if in the last weeks many people are trying to model and fit the official data (GitHub 2020) which are published every day, any attempt of predicting the future development of the pandemic, its peak and the end of it, has failed (Fanelli et al. 2020). Machine learning techniques have been also applied in order to forecast the spreading of the pandemic with similar poor results (Magdon-Ismail 2020). A famous quote attributed to Niels Bohr says “Prediction is very difficult, especially about the future”. That is why in this paper we would like to present a different perspective in order to understand and contain the diffusion of the COVID-19 pandemic, but also to help strategic planning to prevent or contain future epidemics.

The COVID-19 outbreak started officially in China in January 2020, although the virus was probably already circulating in the country since late October 2019 according to a recent report (Giovanetti et al. 2020). In Italy the first infected patient was officially detected on the night of February 20 in Codogno (Lombardia), but a couple of Chinese tourists was hospitalized in Rome (Lazio) already at the end of January after the confirmation test of the infection. So in Italy we have had at least two official starting points of the COVID-19 outbreak: one in the north of Italy and one in the central part (Giovanetti et al. 2020). The latter was spotted even 20 days before, so the question is why the outbreak has spread so rapidly in the northern regions of Italy rather than in the central ones? The question is still unsolved and many think it was simply by chance. However, inspired by a recent position paper (Setti et al. 2020) on the correlation among outbreak diffusion and air pollution, we think we can provide some plausible reasons for this different diffusion and impact of the outbreak by considering several cofactors which differentiate the regions of Italy in various respects. In this paper we propose a novel methodology based on the Crichton's triangle (Crichton 1999, Kron 2002), to perform the epidemic risk assessment of the various regions of Italy in terms of air pollution, people mobility, winter temperature, housing density, health care density and age of the population. We combine all these factors to construct a reliable indicator of the epidemic risk in Italy and we compare it with the impact of current COVID-19 outbreak. We will show that the Italian regions which have been more affected by the pandemic are just the most fragile ones, having the highest risk for a virus epidemic to start, diffuse and be harmful for the population. This will probably mean that the impact on the rest of Italy will not be so severe as in the northern part, at least for what concerns patients in intensive care units (ICU) and deceased ones. We show that our risk assessment compares well also with the official available data of seasonal flu 2019-2020 (Epicentro 2020). Finally we discuss several containment and risk reduction strategies which could be useful not only for the present case, which hopefully will end within a few months, but also in the future to decrease the impact of new epidemic waves.

2 Northern vs Central and Southern Italy: what the official data of COVID-19 outbreak tell us

In what follows, before discussing our new methodology, we would like to discuss the official data released by the Italian Protezione Civile up to April 2 (GitHub 2020), which is the day when we stopped our analysis. Up to April 2 the official report says that in Italy we had 115252 total infected cases and 13915 deceased persons due to COVID-19. However several recent studies have shown that the official data underestimate the correct numbers of infected people. In ref. (Pinotti et al. 2020) it has been shown that at least 60% of infected people do not show almost any symptom and thus these kind of infected are usually not spotted. In fact the testing strategies adopted in Italy have generally consisted in testing only those people who show severe symptoms and especially people over 65 years old. For this reason the daily data officially reported depend very much on the number of tests done on the population and result in a biased sample towards aged patients.

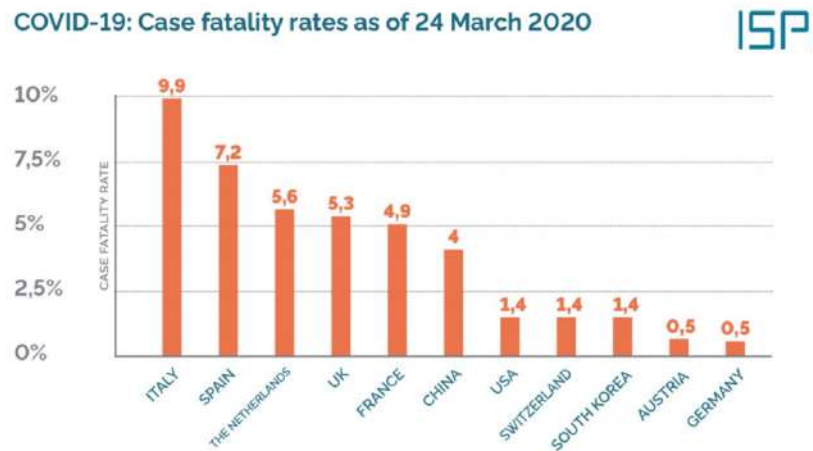


Figure 1: Apparent lethality rate in the various countries, data taken from ISPI report (Villa 2020).

An evidence in favor of this fact is shown in Fig. 1, taken from ISPI report (Villa 2020), where it is reported the apparent lethality rate (i.e. the ratio between the number of deceased patients and the total infected found) recorded in Italy. The average value is the highest in the world with a value around 10%. In China, where the outbreak started, the average value is 4%. Such a disproportion could be also due, in part, to the fact that in China the average age of the population is 38 years old against a value for Italy equal to 47 (Italy is the country with the most aged population after Japan (Worldometer 2020)). However, the main reason is probably related to the fact that the real number of infected people could be much greater than that official data tell us.

It is interesting to notice that the lethality seems to vary a lot also from one Italian region to another. In the right panel of Fig. 2, taken again from (Villa 2020), we show that the apparent lethality rate recorded in the various regions of Italy differs very much when one goes from the northern regions of Italy to the central and southern ones. More in detail, according to the official Italian COVID-19 data, as reported in

ref. (Villa 2020), we have at the moment an apparent lethality rate around 13.6% in Lombardia and around 2.4%, i.e. almost six times less, in Sicilia.

Again, such an increase of lethality in the north with respect to the center and south of Italy, could be related to the number of tests: as shown in Fig.3, the ISPI report (Villa 2020) found an interesting correlation among the apparent lethality rate and the ratio between the number of infected people and the number of tests done. If tests are performed only to severe hospitalized and aged patients, as was done in most of Italian regions with the exception of Veneto, the lethality obviously increases. A plausible realistic estimate of the Italian average lethality rate, according to the ISPI report, can be done through the comparison with other countries and it should be around 1.14%.

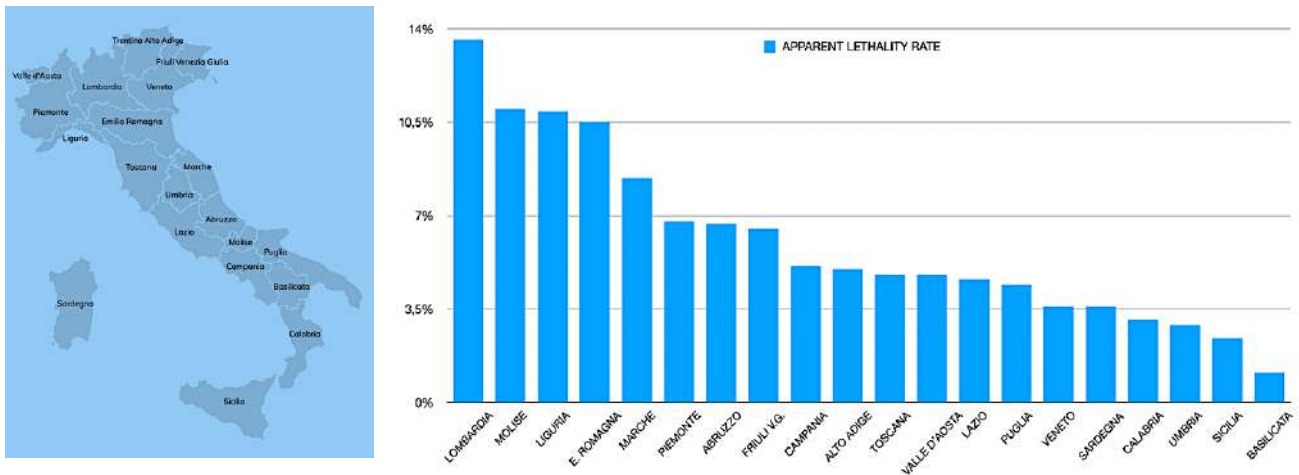
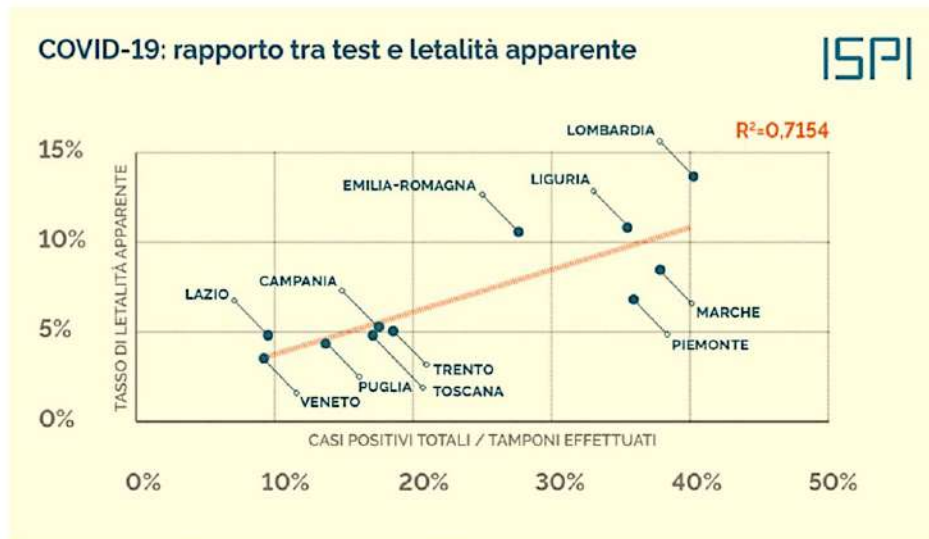


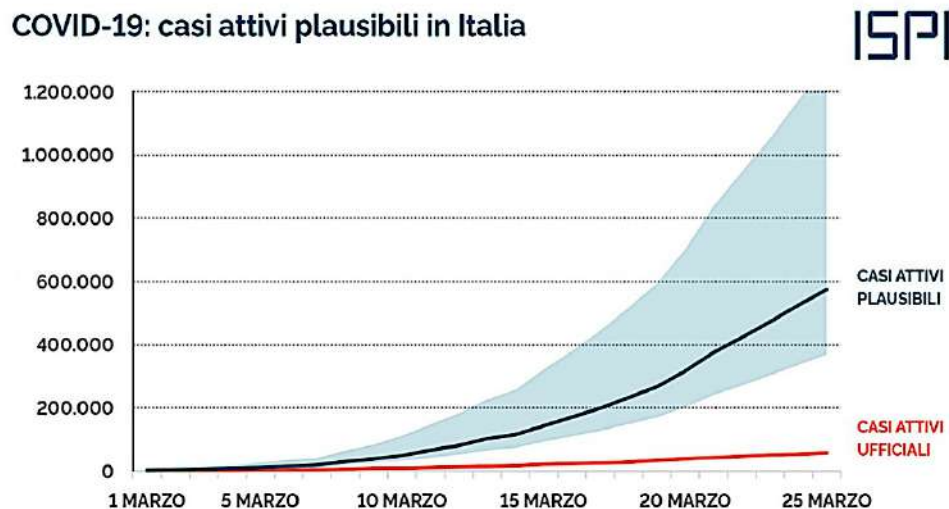
Figure 2: Apparent lethality rate in the various regions of Italy (right panel), data taken from ISPI report (Villa 2020). A geographical map of Italy is also shown for comparison (left panel).



Dati: elaborazione ISPI su dati Protezione Civile

Figure 3: Apparent lethality rate in the various regions of Italy vs the ratio of the total cases with the tests done, data taken from ISPI report (Villa 2020)

On the basis of these data, it is possible to make a more realistic estimate of the actual number of infected people in Italy, which according to the ISPI report should be around ten times the one reported by the official data. The temporal evolution of this more plausible number of real infected people in Italy is plotted in Fig. 4. A recent study of the Imperial College (Flaxman et al. 2020) goes even further along this line, estimating that around 10% of the Italian population (i.e. around 6 million people) has been infected by COVID-19 on March 28, against the official number of around 92500 persons at the same date.



Dati: elaborazione ISPI su dati Protezione Civile

Figure 4: The temporal evolution of the realistic estimate of the number of infected Italian people (black line) compared to that of the official data (red line) according to the ISPI report (Villa 2020)

In the face of such uncertain estimates, in order to have a more reliable indicator of the damages attributable to SARS-CoV-2, it is convenient to look to the average total mortality registered in the various regions. In a recent report of the Italian Health Ministry (MS 2020), the excess of recorded daily deaths (of every kind) observed in the last months has been compared with the average daily numbers calculated, during the same period, in previous years. The report shows an excess of deaths in the last few weeks (beyond one sigma) which in some cases is even 4 times higher than the official COVID-19 data. This can be explained with the fact that many old people, especially in the north of Italy, die in their homes or in their hospices without the possibility to be hospitalized and tested.

But there is another important information that we can extract from these data. In Fig.5, taken from (MS 2020), the report shows the previous data about mortality disaggregated between northern and central-southern part of Italy: while for the northern regions (top panel) the excess of mortality is clearly visible, representing the contribution related to coronavirus epidemics, in the central and southern part of the country (bottom panel) the data do not reveal (at 28 of March) such a strong discrepancy from the annual average.

Summarizing, we can conclude that, in general, the official Italian data on the COVID-19 outbreak which are available at the moment heavily underestimate the correct ones, but we do not know how much they do this and how much they are biased towards (more aged) patients which present more severe symptoms.

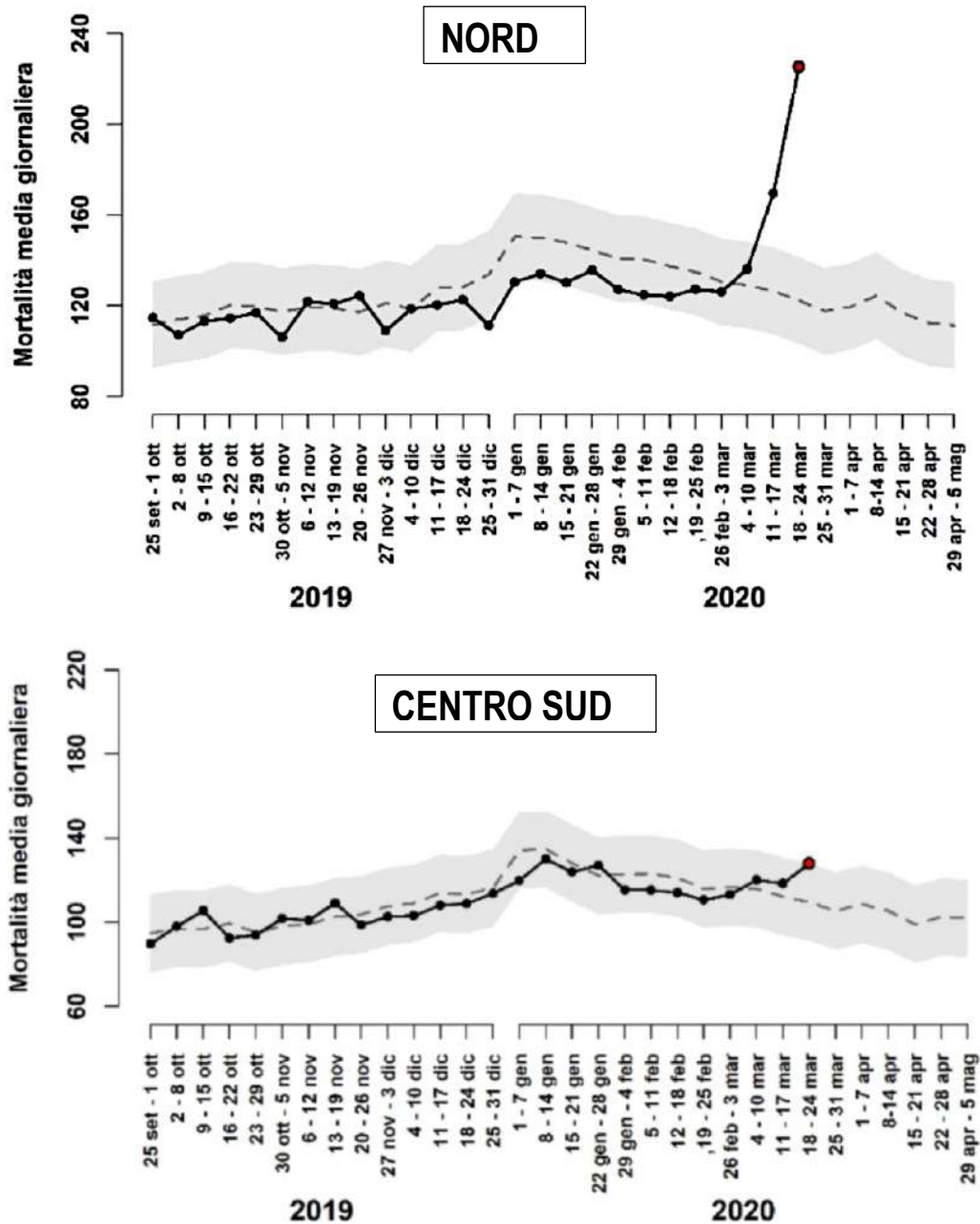


Figure 5: Average daily mortality (full line) in the north (top panel) and in the central and south (bottom panel) of Italy, from 25/09/2019 to 24/03/2020, compared with the average daily mortality registered in the same period in previous years (dashed line); see ref. (MS 2020).

On the other hand, if the official data on COVID-19 outbreak in Italy do not give a clear scenario of the actual impact that the outbreak is having on the country, this also implies that it is very unlikely that by using standard models based on the absolute values of these data, one could predict in an accurate way the peak of the outbreak or its ending (see e.g. Fanelli et al. 2020, Magdon-Ismail 2020). The only thing that clearly emerges without any doubt from the data we have shown, and in particular from those of figure 5, is that the impact of the outbreak in the northern regions of Italy is for sure much more dramatic than in the rest of the country. This is certainly strange if one considers that, as already clarified in the introduction, in Italy we have had at least two official starting points of the COVID-19 outbreak, one in the central part (at the end of January) and one in the northern part (at the end of February) (Giovanetti et al. 2020), with several waves of hundreds of thousands people leaving the northern areas to come back to the original incoming regions of central and southern areas before the lockdown of the country on March 9 (Pepe 2020). Therefore with very high probability the contagion had enough time for spreading almost homogeneously in all the regions, already before any mobility restriction, and probably had it. However, it seems that, for some reason, the epidemic effects – both in terms of total cases and deaths – have been amplified in a limited number of regions. We believe that, if one maintains an aggregate approach at the level of groups of regions, notwithstanding the limitations and underestimation stressed above, the official COVID-19 data still contain useful information to explain this anomaly.

In the following sections we propose a data driven methodology able to assess the *a-priori* risk level affecting the different Italian regions with respect to a generic epidemic flu with some features in common to those of the COVID-19. We will show that this general analysis is already able, at a first level of approximation, to account for the asymmetric diffusion and impact of the COVID-19 outbreak in Italy. Later on, making use of the COVID-19 official data (up to April 2), we will further calibrate our method in order to improve the risk ranking for the Italian regions. A similar analysis could be replicated for any other country in the world, in order to verify if the *a-priori* risk ranking of different regions would match with the observed damage ranking of COVID-19.

3 Risk Assessment framework

Conventional risk assessment theory relies on “Crichton’s Risk Triangle” (Crichton 1999, Kron 2002) (Fig. 6). Risk is evaluated as a function of hazard, exposure and vulnerability. All three variables are required to co-exist in the same place to assess the presence of a risk. A hazard is the potential of an event to cause damage (e.g. earthquakes, flooding, epidemics), exposure is a measure of assets exposed to the potential damage (e.g. buildings, infrastructures, people), vulnerability is the attitude to be harmed when exposed to the event (e.g. building characteristics, drainage systems, age). Hazard and exposure share the same geographical location. Used for the first time in the insurance industry (Crichton 1999), this approach has been extended to assess spatially distributed risks in many fields of disaster management: the impact on health of the urban heat island effect due to climate change (Tomlinson et al. 2011) (IPCC 2014), the disaster risk reduction related to climate change in general (Thomalla et al. 2006) (Kim et al. 2015) (Collins et al. 2009) or to earthquakes (Babayev 2010)



Figure 6: An example of Crichton’s Risk Triangle.

For the purpose of this paper, hazard is the probability that a virus can potentially spread among the population of a given territorial district. We will consider the 20 regions of Italy. We do not consider the transitory phase during which the virus spreads, from its initial spark, to the whole Italian territory; therefore the initial level of spreading of the virus is supposed quite homogeneous all over the regions, but, its potential to be transmitted among people living in the same area, that is the extension of the infection, is increased as a result of a set of factors, related to spatial and socio-economic characteristics of people living in the region. With these premises the hazard will be named “*Infection Diffusion*”, while the *Exposure* essentially coincides with the size of the population of each region, which represents the amount of people who might potentially be sick from the infection.

The third component of the epidemic risk, *Vulnerability*, represents the attitude of an infected person to become sick or die; it is a kind of relationship between a stimulus (the infection) and the health damage resulting; it can be seen as a the probability to be sick after an infection or the degree of damage when a

person is exposed to the hazard. It is strongly related to the age and initial health conditions before the infection. Vulnerability can be combined with exposure, to obtain a measure of the absolute damage, i.e. the number of people in a given region who become ill for pathologies related to the virus, which will be called *Consequences*.

As we will see in detail in the next section, the three components of the risk can be quantitatively estimated, for each region, using a proper combination of several variables or risk indicators. In the following, we present these indicators explaining the rationale under their choice, which relies on either generic epidemics literature or recently confirmed features of the COVID-19 outbreak. Of course many other possible indicators could have been selected, but at the moment we decided to restrict our analysis to those we consider the most relevant.

INFECTION DIFFUSION

Mobility index

Commuting data are often used to correlate population mobility and the spreading of an infection (Charaudeau et al. 2014). According to available data, 84.50 % of the Italian population in the age range 14-80, make at least one trip per typical weekday, the average trip rate is 2.50 per day, the average distance covered is 28.5 km per day, while the distribution of the distance per each trip is 28% is less than 10 km, 38% in the range 10-50 km and 34% over 50 km (ISFORT 2019). Assuming constant the trip rate all over Italy, we consider a “mobility index” as the ratio between the sum of commuting flows (incoming and outgoing) for municipality and the population employed in the municipality (mobility index for each region is the average of the values of all its municipalities).

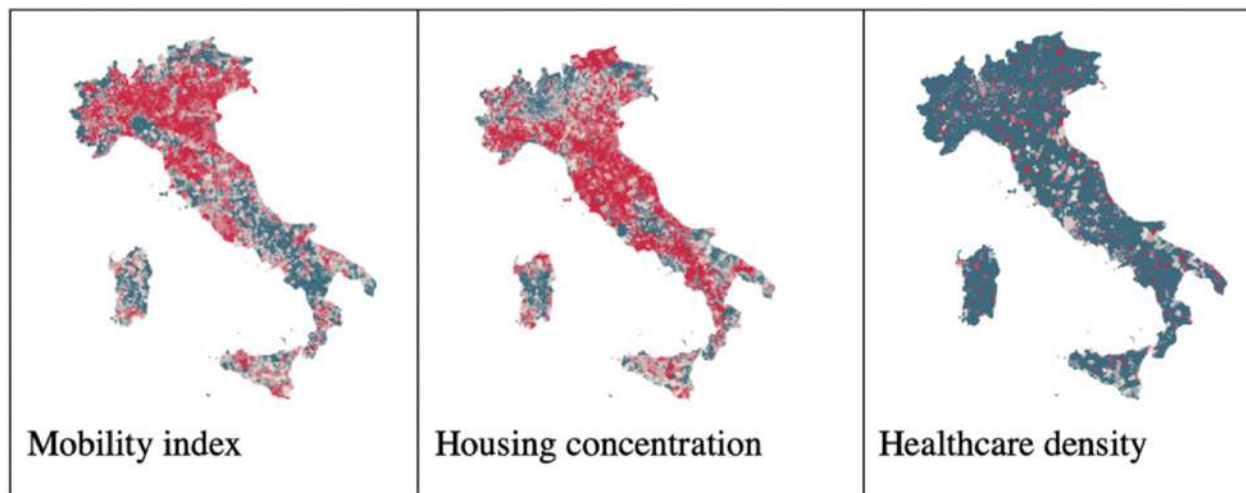


Figure 7: Maps of some of the indicators described in the text at the urban level (Source: <https://www.urbanindex.it/>).

The source of mobility index and the other statistical indicators cited hereafter (housing concentration, healthcare density and population) and the relative infographics of Fig. 7 is a dataset made available by the Italian Department for Economic Policy Planning and Coordination (www.urbanindex.it). Data, that are provided at the municipality scale in the dataset, were aggregated as regional average.

Housing concentration

Urbanization increasingly affects the epidemiological characteristics of infectious disease (Alirool et al. 2011). Close proximity of people in their short range mobility and the attitude to use crowded public transportation is amplified in compact and dense cities. We included the Housing Concentration as a variable to capture those circumstances, measured as the ratio between the total number of houses and the number of houses classified as "detached houses".

Healthcare density

Recent studies have shown that not all infected individual within a population have equal chances of transmitting the infection to others. Some individuals infect disproportionately more secondary contacts, as compared to most others (Stein 2011). Delayed hospital admission, misdiagnosis, unsuitable air conditioning systems, lack of infected patients segregation and inter-hospitals transfers, all might contribute in what it is commonly called super-spreading event.

We measure the potential occurrence of this events in the infection spreading including a descriptive variable for each region the Healthcare Density as the number of hospital beds per inhabitant.

EXPOSURE

We measure the exposure by the presence of people that could be affected by the infection. As anyone who is infected might get ill, we use the total population of each region.

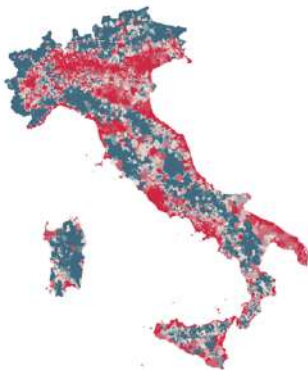


Figure 8: Map of urban population (Source: <https://www.urbanindex.it/>).

Looking to Fig. 8, it is worth to notice the uneven distribution of the population among the regions and the different geographic areas. About 43% of the population is concentrated in the five regions of Northern Italy (Valle d'Aosta, Piemonte, Lombardia, Veneto, Friuli, Trentino) and one out of six in Lombardia, In Southern Italy the population is mostly concentrated along the coastal areas.

VULNERABILITY

Pollution

Concentration of particulate matter (PM) above the EU daily limits were registered at 22% of the reporting station in 17 of the 28 EU Member States in 2017 (www.eea.europa.eu). Similar situations relates to other air pollutants such as ozone, nitrogen dioxide and many others, all impacting human health, particularly lower socio-economic group, children, older people and those with pre-existing health conditions. PM concentration in 2016 were responsible for about 374.000 premature deaths in the EU-28, 68.000 for exposure to NO₂ and 14.000 to O₃.

We use the pollution indicator that measures the regional average of the number of days of exceeding the limit for the protection of human health for PM₁₀ in the provincial capitals in 2018. Data can be found in ISTAT databases (<https://www.istat.it/it/archivio/aria>).

This factor has been used for the calculation of the vulnerability component of the risk index because people with chronic lung and heart conditions caused or worsened by long-term exposure to air pollution are less able to fight off lung infections and more likely to die (Cui et al. 2003).

Temperature

The possibility that weather plays a role in the spread of 2019-nCoV is worth to be investigated (Bukhari and Jameel 2020), because the question is still controversial.

A research on the SARS Coronavirus in 2011(Chan et al. 2011) reports that low temperature and low humidity environment may facilitate the virus transmission in community in subtropical area during the spring and in air-conditioned environments. It is also commonly accepted that cold cut down the defense barriers of the respiratory tracts, while social distance is shortened by the full sharing of closed environments (Chowel et al. 2012).

In general when the average temperature drops by 1°C the estimated risk for the lower respiratory tract infections is 2.1% (OR 1.08, 95% CI 1.0; 1.04, p=0.038) (Makinen T.M. et al. 2009). Italy experiments a wide difference of climatic zones with much lower temperature in northern regions compared to

southern ones; therefore we decided to include the average winter (from December 2016 to April 2017) mean temperature in each region as a factor potentially enhancing the individual vulnerability. The source of data is the Italian Ministry of Agriculture (<https://www.politicheagricole.it/>).

Aged population

Most of the official data sources report more severe impacts of 2019-nCoV on elderly people, probably both for an intrinsic weakness of their immunity system and for the co-existence of other chronic pathologies. We use the ratio between the population over 60 and the total population to take into account this vulnerability factor.

4 Data Analysis and Results

In this section we will describe in detail how to calculate and aggregate the three risk components in order to derive our global risk index and to build a risk ranking for the Italian regions. Then we will use it for exploring the correlations between this ranking and the observed effects of the COVID-19 outbreak.

In the previous section we motivated the choice of the reference variables (risk indicators) that we adopt here to derive the three risk components as summarized in Fig.9. As already clarified, exposure and vulnerability can be also considered aggregated in the variable consequences.

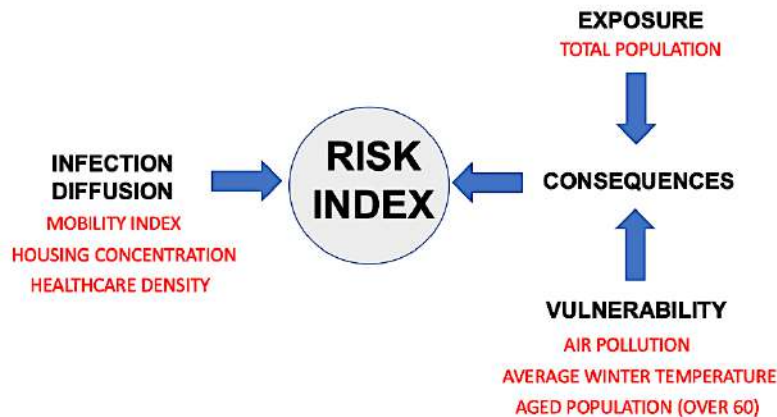


Figure 9: Variables (risk indicators, in red) that contribute to the three components (in black) of the Risk Index.

Let us briefly show, first, to what extent these variables individually correlate with the main damages indicators of the COVID-19 epidemic, detected in each Italian region up to April 2 2020 (data from GitHub Repository COVID-19 2020). In particular, in Fig. 10 we report the number of total cases of infected individuals versus the three variables aggregated in the infection diffusion (mobility, housing concentration and healthcare density), being the latter more related with the contagion extension. On the other hand, in Fig. 11, the number of deaths are plotted as function of the variables which enters both in the exposure (population) and in the vulnerability (air pollution, average winter temperature and aged population), since these indicators are more related with the possible severe consequences of having been infected. From now on, data of the autonomous districts of Trento and Bolzano will be aggregated in the region Trentino Alto-Adige.

From a quick look to the various panels of both figures, it clearly appears that the regions belonging to the northern part of Italy, and Lombardia in particular, which today seem to be more exposed to the contagion and suffers more deaths with respect to the southern regions, in several cases record quite high values of the risk indicators (plots are in semi-log scale for a better visualization; the color of the circles in all the plots does scale with the total population of the corresponding regions).

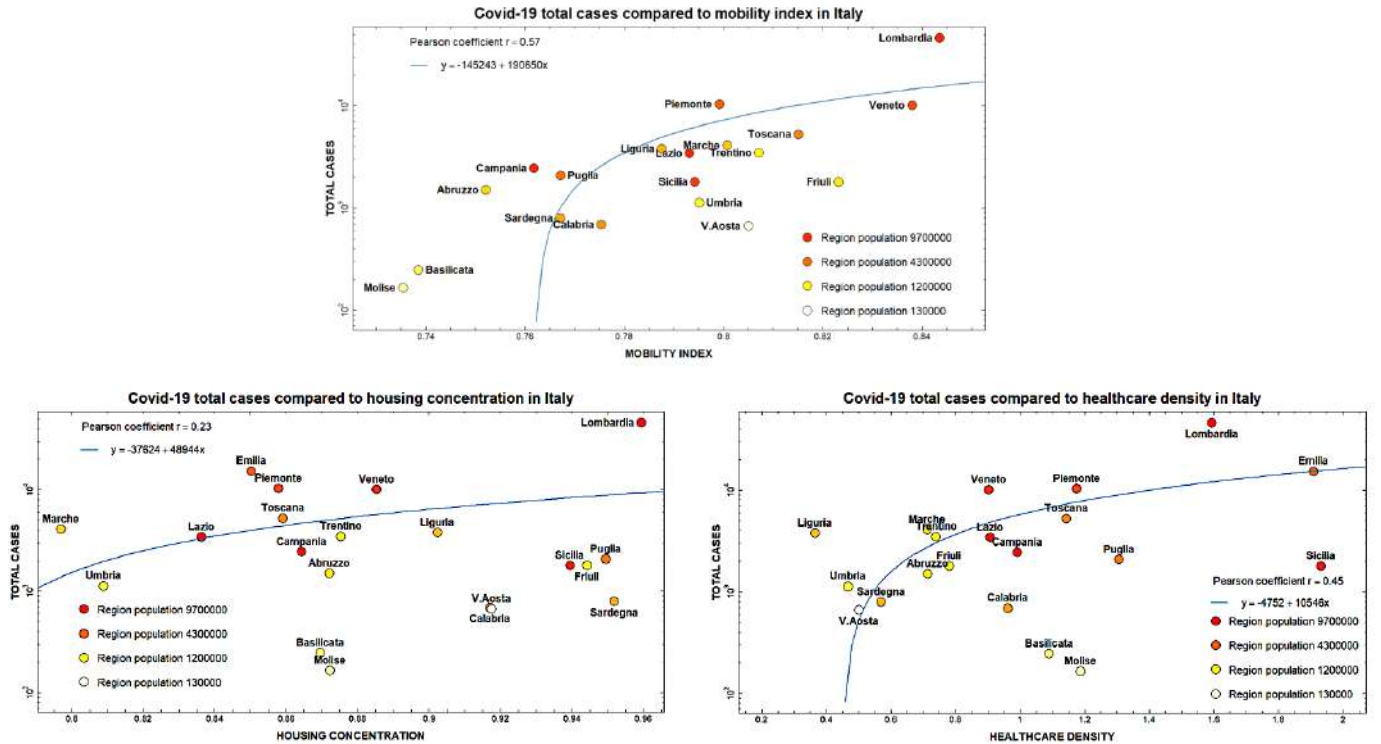


Figure 10: The number of total cases of infected people are reported, in a log-lin scale, versus our risk indicators of infection diffusion for all the Italian regions updated at April 02 2020. The color intensity is proportional to the total population of each region. A linear fit is also shown, see text.

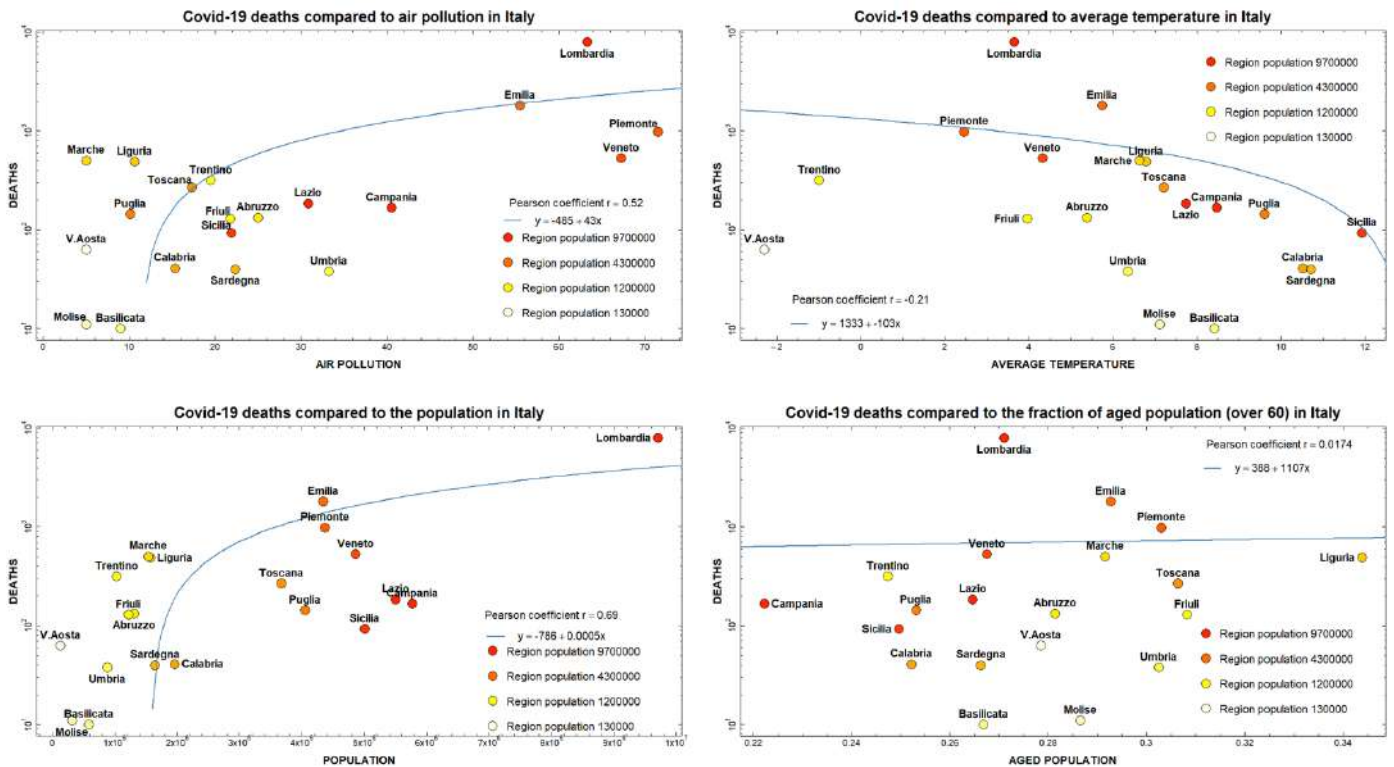


Figure 11: The number of deaths are reported, in a log-lin scale, versus our risk indicators of infection diffusion for all the Italian regions updated at April 02 2020. The color intensity is proportional to the total population of each region. A linear fit is also shown, see text.

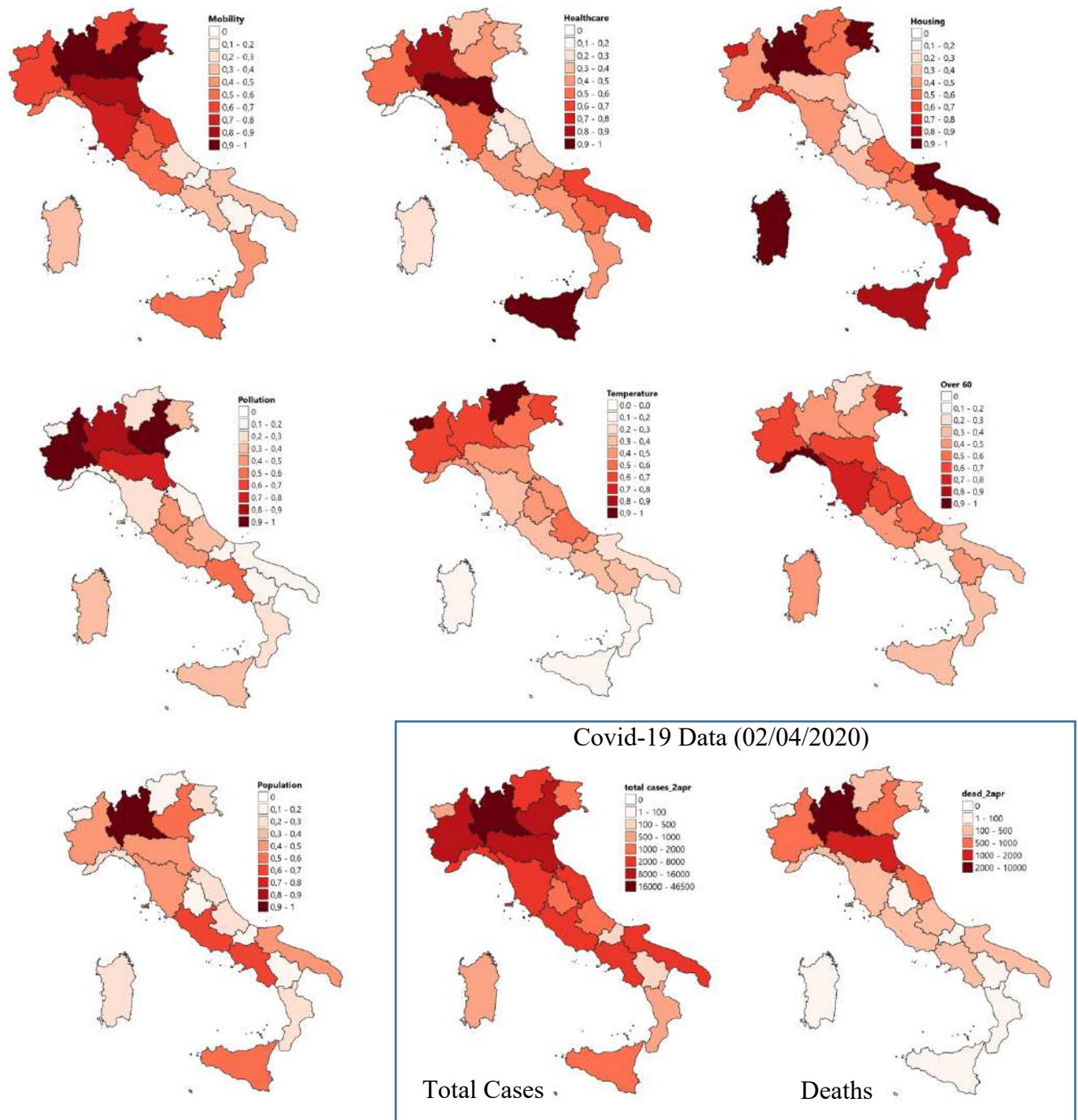


Figure 12: (a) The geographical distribution of our risk variables (indicators) in color scale for the various Italian regions is compared with the geographical distribution of the damages (total cases and deaths), calculated at 26/03/20 (the two panels are boxed at the bottom-right). A concentration of dark colors in the northern regions is roughly visible for all the indicators.

It appears that, in general, the correlation of each single variable with the COVID-19 damages is quite poor. This is evident looking at the low values of the Pearson coefficients of the simple linear fits present in each plot and it is also visually confirmed by the comparison between color maps in Fig.12 (where the variables have been normalized between 0 and 1, ordered according to an increasing risk level). Therefore, an appropriate combination of these indicators seems to be strongly advisable.

A better agreement with the COVID-19 data would be of course obtained by fitting them with some given aggregation model. In this section we will proceed along this direction in three steps. First, we will adopt COVID-19 data in order to verify if the proposed model of grouping the variables in the three main risk components summarized in Fig.9 is a good choice with respect to other possibilities. Then, we will use a *parameter-free* version of the model for obtaining an *a-priori* risk ranking for the considered regions, potentially adaptable to other countries or to other epidemic datasets (for viruses to some extent compatible with the basic features of COVID-19, like e.g. the seasonal flu). Finally, we will apply the same model to the specific COVID-19 outbreak by using the fitting parameters obtained by minimizing the error with respect to the total cases observed at April 2 2020 and comparing the resulting (*a-posteriori*) risk ranking with the *a-priori* one.

4.1 Calculation of the Risk Index and verification of the IEV model

We observe that, in any model, the risk has to be necessarily proportional to the exposure, represented by the population, therefore we will assume that the risk is given by the product of the exposure times a given function F_{IV} of the other parameters:

$$R = (E * F_{IV}) (params)$$

The seven parameters under consideration are listed below, together with their reference interval:

Population:	$X_0 \in [126806, 9704151]$
Mobility index:	$X_1 \in [0.73, 0.84]$
Housing concentration:	$X_2 \in [0.79, 0.96]$
Healthcare density:	$X_3 \in [0.36, 1.93]$
Air Pollution:	$X_4 \in [5.00, 71.00]$
Average mean Temperature:	$X_5 \in [-2.29, 11.92]$
Aged Population (fraction of over-60 individuals):	$X_6 \in [0.22, 0.34]$

These variables are suitably normalized between zero and one as:

$$x_0 = \frac{X_0}{\max(X_0)} \quad ; \quad x_i = \frac{X_i - \min(X_i)}{\max(X_i) - \min(X_i)}, \quad i = 1, \dots, 6$$

where $\min(X_i)$ and $\max(X_i)$ are, respectively, the minimum and the maximum value assumed by each variable X_i in its own reference interval. The new normalized variables are also dimensionless.

Assuming an a-priori multiplicative role of the population x_0 , the simplest form of the dependence of the function F_{IV} would be the linear one, so we could consider:

$$R_{E_{IV}} = E * F_{IV}$$

$$E = x_0 ; F_{IV} = c_{IV} + \alpha_1 x_1 + \dots + \alpha_6 x_6$$

where $c_{IV}, \alpha_1, \dots, \alpha_6$ are fitting parameters.

We shall call this E_IV model, because infection diffusion and vulnerability are somehow combined together in a single function that depends linearly on the parameters.

On the other hand, according to the risk assessment theory relying on ‘‘Crichton’s Risk Triangle’’ introduced in the previous section, we may assume that F_{IV} is the product of infection diffusion and vulnerability, i.e.:

$$R_{E_{IV}} = E * F_{IV} = E * I * V \quad (1)$$

$$E = \alpha_0 x_0 \quad (2)$$

$$I = c_I + \alpha_1 x_1 + \alpha_2 x_2 + \alpha_3 x_3 \quad (3)$$

$$V = c_V + \alpha_4 x_4 + \alpha_5 x_5 + \alpha_6 x_6 \quad (4)$$

Let us call this model E_I_V. Again, $c_I, c_V, \alpha_0, \dots, \alpha_6$ are fitting parameters.

We shall compare the two models by performing a fit with the COVID-19 data available. In particular, we shall perform a nonlinear least square best-fit, by trying to fit the total number of cases in each region up to April 2, 2020. Because in the E_I_V model the dependence of the risk on E, I and V is multiplicative, we may add two normalization conditions in order to avoid infinite solutions, for example:

$$\alpha_1 + \alpha_2 + \alpha_3 = 1 \quad (5)$$

$$\alpha_4 + \alpha_5 + \alpha_6 = 1 \quad (6)$$

For both models, we shall minimize the error:

$$\mathcal{E}^2 = \sum_{k=1}^n \left(C_k - E_k * F_{IV}(x_1^{(k)}, \dots, x_6^{(k)}; params) \right)^2$$

with respect to the parameters. In this expression $n = 20$ is the number of regions, C_k denotes the number of cases for region k , E_k indicates the population of region k , and the function F_{IV} depends on the model considered.

The relative mean quadratic error ε is defined as

$$\varepsilon^2 = \frac{\varepsilon^2}{\sum_{k=1}^n (C_k)^2}$$

We perform the minimization of the error by adopting the Levenberg-Marquardt algorithm, using Matlab® Optimization Toolbox™.

The results of the best-fit with the two models are the following:

- 1) Model E_IV (where the effect of infection and vulnerability are combined in a single affine function of the parameters): $\varepsilon = 0.313$
- 2) Model E_I_V (where the infection diffusion depends only on mobility index, housing concentration, healthcare density, while vulnerability depends only on average mean temperature, air pollution and aged population): $\varepsilon = 0.108$

This first result confirms that the choice of the model E_I_V is preferable to the E_IV one, since it produces a lower error with respect to real COVID-19 data.

It is important to notice that in model E_I_V the sign of the coefficients α confirm that the correlation of infection diffusion on mobility index, housing concentration, healthcare density is positive, and so is the correlation of vulnerability on air pollution and aged population, while vulnerability correlates negatively with the average mean temperature, as one could expect since – as explained in section 3 – low temperatures cut down the defense barriers of the respiratory tracts increasing the risk of being injured by the virus. For this reason, in order to simplify the normalization of the coefficients, we decided to replace the normalized temperature x_3 by a new variable $\tilde{x}_3 = 1 - x_3$, so that the new variable is still in the interval $[0,1]$, but now the corresponding coefficient α_3 will be positive (in this way the minimum temperature has $\tilde{x}_3=1$ – max risk – and the maximum temperature $\tilde{x}_3 = 0$ – min risk).

4.2 General version of the E_I_V model and a-priori risk ranking

Once confirmed the convenience to adopt the E_I_V model, let us now build an approximated *a-priori* risk ranking composing together the three components E, I and V defined in equations 2-4, assuming that all the variables would contribute with the same weight to each component. In particular, taking also into account the normalization conditions of equations 5-6, we set:

$$c_I = 0, c_V = 0 ; \alpha_0 = 1 ; \alpha_i = \frac{1}{3}, i = 1, \dots, 6$$

This choice makes, at this stage, our estimation of the regional risk independent of any specific epidemic flu. We will compare this ranking with the damage ranking of the COVID-19 data, both in terms of total cases and deaths, as an example.

By multiplying exposure and vulnerability for the k -th region we recover the Consequences:

$$C_k = E_k \cdot V_k \quad (k=1, \dots, 20) \quad (7)$$

Then, by multiplying infection diffusion and consequences, we finally obtain the global risk index R_k for each region:

$$R_k = I_k \cdot C_k \quad (k=1, \dots, 20) \quad (8)$$

In this respect, the risk index can be interpreted as the product of something related with the causes of the virus diffusion (I_k) and something related with the effects on the individuals (C_k).

In Fig. 13 we give a first look to the ranking of Italian regions disaggregated for the two main risk components, i.e. the infection diffusion (related to the causes of epidemic diffusion) and the consequences (related to the effects of that diffusion), both normalized to their maximum values so that Lombardia has $I_k=C_k=1$. One can notice that a quite rough separation between northern regions (with higher scores) and those of center and south (with lower scores) can be already appreciated in these two rankings.

Ranking	Infection Diffusion	Ranking	Consequences
Lombardia	1,00	Lombardia	1,00
Sicilia	0,87	Piemonte	0,56
Emilia Romagna	0,76	Veneto	0,50
Friuli Venezia Giulia	0,71	Emilia Romagna	0,43
Veneto	0,66	Lazio	0,31
Puglia	0,66	Campania	0,25
Toscana	0,58	Toscana	0,25
Calabria	0,54	Sicilia	0,13
Piemonte	0,53	Liguria	0,13
Valle d'Aosta	0,53	Puglia	0,11
Trentino Alto Adige	0,50	Friuli Venezia Giulia	0,10
Sardegna	0,49	Abruzzo	0,09
Liguria	0,41	Marche	0,08
Lazio	0,40	Trentino Alto Adige	0,08
Campania	0,38	Umbria	0,07
Molise	0,35	Sardegna	0,06
Basilicata	0,34	Calabria	0,05
Abruzzo	0,30	Basilicata	0,02
Marche	0,30	Molise	0,02
Umbria	0,25	Valle d'Aosta	0,01

Figure 13: Ranking of Italian regions according to infection diffusion (on the left) and consequences (on the right) in the parameter-free case, see text.

On the other hand, as expected, in order to improve the correlation with real epidemic damages, for example those observed for COVID-19, we need to put together I and C in the global risk index (8). This is visually anticipated in Fig. 14, where the color maps of the geographical distribution for infection diffusion and consequences (at top) are presented together with the color map (at bottom) of the *a-priori* risk index, whose detailed ranking is reported in the next figure.

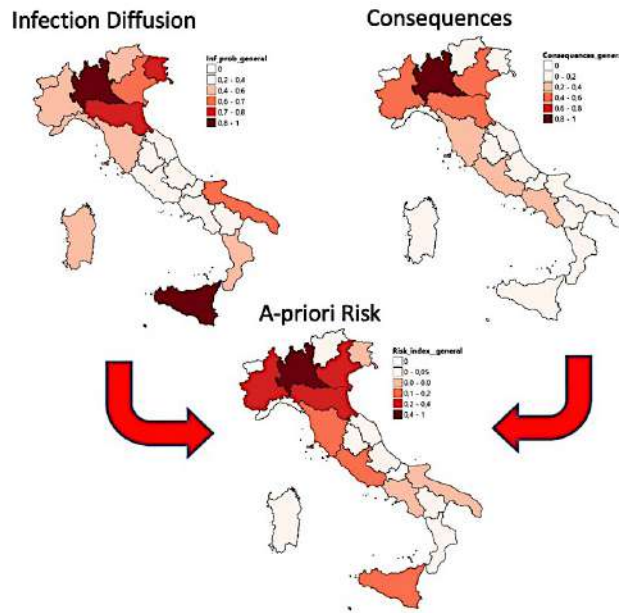


Figure 14: Color geographic maps of infection diffusion and consequences (top maps) compared with the global *a-priori* risk map (bottom map).

In Fig. 15 we can finally appreciate the predictive power of the *a-priori* risk ranking of the Italian regions, compared with the COVID-19 data about total cases and deaths up to April 2 2020. The values of R_k have been normalized to their maximum value, so that Lombardia results to have $R_k=1$ (as also visible in the map of Fig.14). The average of R_k over all the regions results to be $R_{av} = 0.14$ and can be considered approximatively a reference level for the Italian country (even if, of course, it has only a relative value). As already explained, due to the intrinsic limitations of the official COVID-19 data, it is convenient to make the comparison at the aggregate level of groups of regions. Let us therefore arrange the 20 regions in 4 groups, depending on their level of a-priori risk (less than 0.03, between 0.03 and $R_{av} = 0.14$, between 0.14 and 0.5, more than 0.5). With this choice, our model is able to correctly identify the northern regions where the epidemic effects are today far more evident: the first in the ranking, i.e. Lombardia (with a risk score about three times more than the second classified) and the group of the three regions immediately after it, Veneto, Emilia Romagna and Piemonte (even if not in the exact order of damage). A quite good agreement can be observed also for the other two groups. Only in two cases, Sardegna and Calabria, the effects on both total cases and deaths have been overestimated, while for other two regions, Marche and Umbria, they have been underestimated. Also Valle d'Aosta was underestimated, but limited to the deaths.

Ranking	A-priori Risk Index	Total Cases	Deaths
Lombardia	1,00	46065	7960
Veneto	0,33	10111	532
Emilia Romagna	0,32	15333	1811
Piemonte	0,30	10353	983
Toscana	0,14	5273	268
Lazio	0,13	3433	185
Sicilia	0,12	1791	93
Campania	0,09	2456	167
Friuli Venezia Giulia	0,07	1799	129
Puglia	0,07	2077	273
Liguria	0,05	3782	488
Trentino Alto Adige	0,04	3482	187
Sardegna	0,03	794	40
Calabria	0,03	691	41
Abruzzo	0,03	1497	133
Marche	0,02	4098	503
Umbria	0,02	1128	38
Basilicata	0,01	246	10
Valle d'Aosta	0,01	668	63
Molise	0,01	165	11

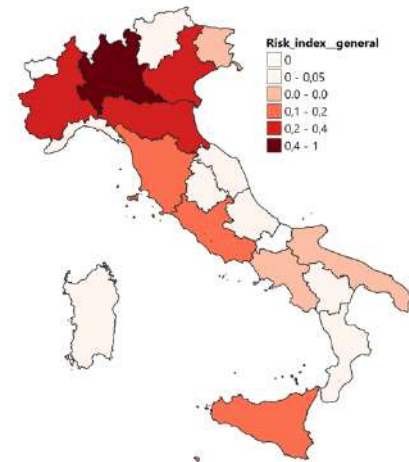


Figure 15: *A-priori* normalized risk ranking of Italian regions, emerging from our analysis of risk indicators, compared with the corresponding total cases and deaths updated at April 2, 2020. The average risk over all the regions is $R_{av} = 0.14$. On the right, the geographical distribution of risk is reported again for comparison.

These discrepancies suggest at least two opposite explanations, both plausible: (1) assuming that the proportions of damages in the various regions will stay more or less the same until reaching the epidemic peak, it could be possible that some important risk indicator was neglected in building the components of the global risk index, or – as expected – (2) it is likely that the weights α_k of the current indicators (chosen here equals as a first approximation) would require a fine tuning through a fitting procedure on real epidemic data. As anticipated, we will follow this last road in the next paragraph.

To further support the good agreement between the *a-priori* risk ranking and the observed data, in Fig. 16 we show the correlations between the risk index and the three main indicators of damage related to COVID-19, i.e. the total number of cases, the total number of deaths and the intensive care occupancy. For each plot, a linear regression has been performed taking into account only the first 10 regions in the ranking (in the left column) and all the regions in the ranking (right column). The Pearson correlation coefficient always takes values greater than 0.95, indicating a strong positive correlation. Of course the fits with only the first 10 regions give back slightly better correlation coefficient values.

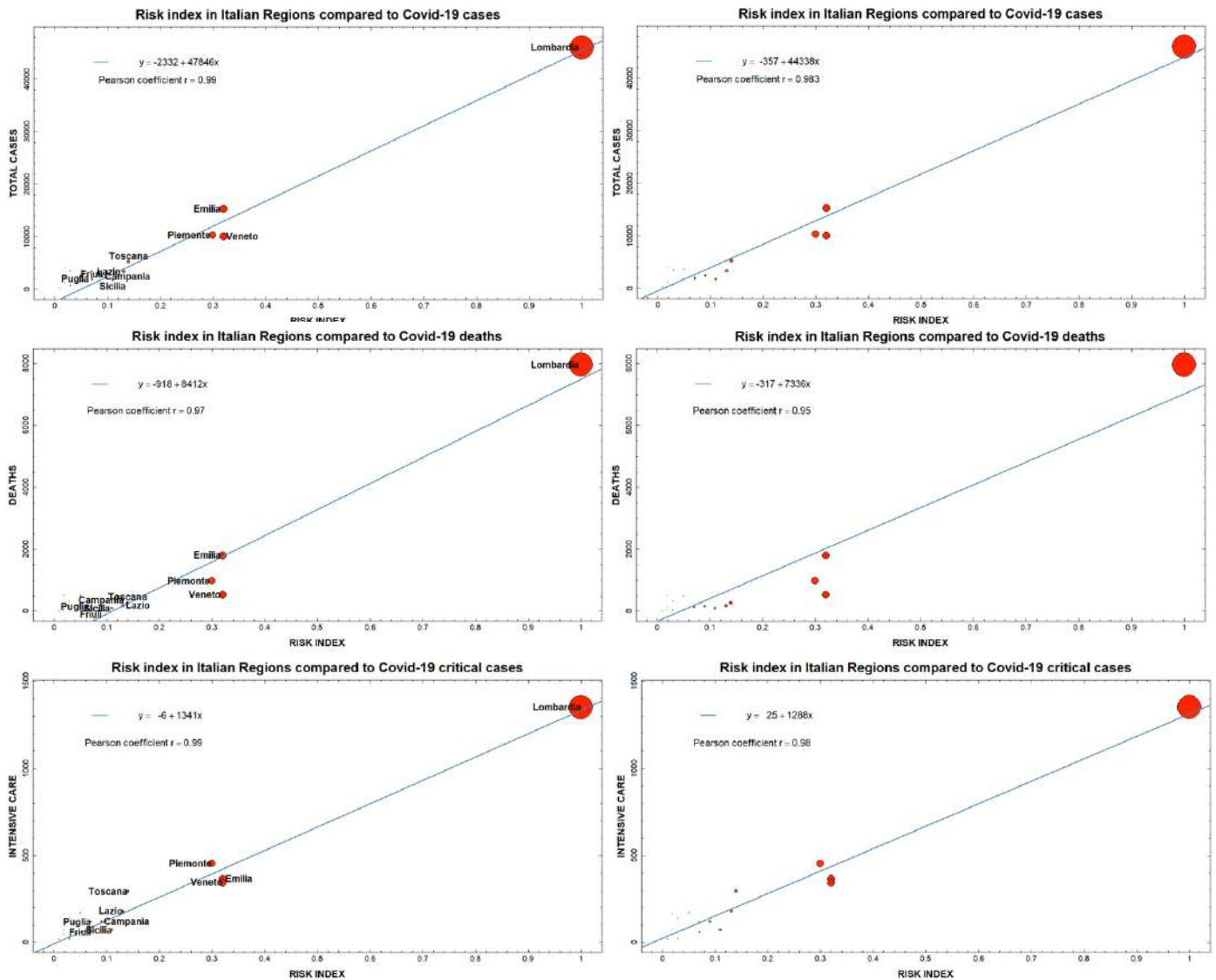


Figure 16: The three main damage indicators, updated at April 2, 2020, are reported as function of our a-priori risk index for all the Italian regions. The size of the points is proportional to the risk index score. A linear regression has been performed for each plot, only for the first 10 regions in the ranking (left column) and for all the regions in the ranking (right column). The Pearson correlation coefficients are in both the cases very good, always greater than 0.95, even if slightly better when only the first 10 regions are considered in the fit.

In the next paragraph we will try to improve the predictive power of our E_I_V model by adapting it to COVID-19 data. As a last remark, we notice again that our *a-priori* model is also able to identify the most risky regions without reference to the specific flu epidemic. This is confirmed by Fig.17, where the risk map (middle panel) is compared with both the map of COVID-19 total cases (left panel) and the map of the serious cases and deaths (right panel) of the seasonal flu 2019/2020 in Italy (ISS data, Epicentro 2020).

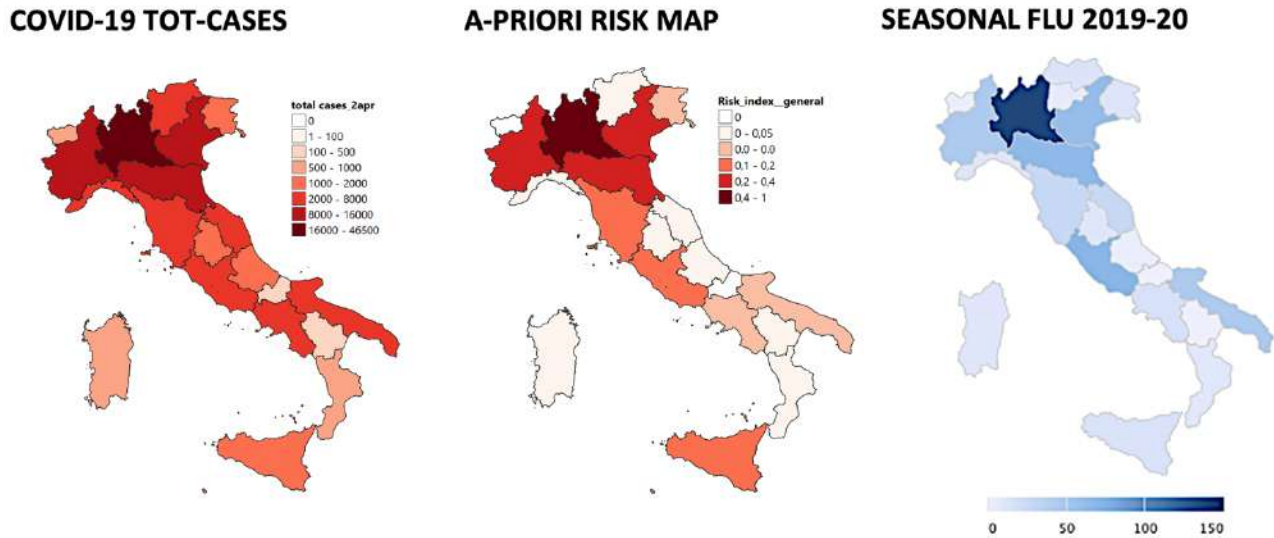


Figure 17: Comparison between the spatial distribution of COVID-19 total cases (left panel), the regions most struck (in terms of severe cases and deaths) from 2019-2020 seasonal flu (right panel) according to the ISS data (Epicentro 2020) and our *a-priori* risk map (central panel). The geographical correlation with the risk map is evident for both the epidemic flus.

The agreement is already visible at a first sight, but it could be made more stringent through a more detailed analysis based on regional historical data about seasonal flu in the previous years (this will be the subject of another study, currently in progress).

4.3 Application of the E_I_V model to COVID-19 and *a-posteriori* risk ranking

In this last paragraph of section 4 we repeat the previous risk analysis but calibrating the weighting parameters of the E_I_V model through a nonlinear least square best-fit procedure on the official COVID-19 data about total cases, like in the first paragraph. Taking again into account the normalization conditions (5-6), we found the following values for the weighting coefficients of equations 3-4:

I	V
$c_I = -0.1670$	$c_V = 0$
$\alpha_1 = 0.2820$	$\alpha_4 = 0.8186$
$\alpha_2 = 0.2137$	$\alpha_5 = 0.1350$
$\alpha_3 = 0.5093$	$\alpha_6 = 0.0464$

The quantity E of equation 2 is obtained by multiplying the population by a coefficient $\alpha_0 = 1.1166 * 10^5$. The product $R = E * I * V$ will then give the best fit for the total number of observed cases.

Ranking	A-posteriori Risk Index	Total Cases	Deaths
Lombardia	1,00	46065	7960
Emilia Romagna	0,32	15333	1811
Piemonte	0,25	10353	983
Veneto	0,25	10111	532
Toscana	0,13	5273	268
Lazio	0,09	3433	185
Puglia	0,07	2077	273
Friuli Venezia Giulia	0,07	1799	129
Campania	0,06	2456	167
Trentino Alto Adige	0,05	3482	187
Sicilia	0,04	1791	93
Liguria	0,02	3782	488
Calabria	0,02	691	41
Marche	0,02	4098	503
Abruzzo	0,01	1497	133
Sardegna	0,01	794	40
Basilicata	0,01	246	10
Valle d'Aosta	0,01	668	63
Molise	0,01	165	11
Umbria	0,00	1128	38

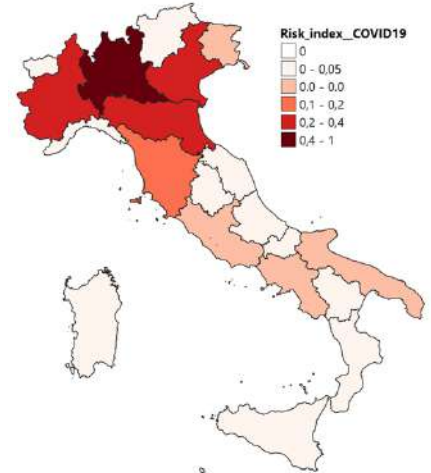


Figure 18: *A-posteriori* normalized risk ranking of Italian regions, calculated through an optimization of the E_I_V model with COVID-19 official data, compared with the corresponding total cases and deaths updated at April 2, 2020. The average risk over all the regions is now $R_{av} = 0.12$. On the right, the geographical distribution of risk is reported in a colored map.

Using this adapted model, the *a-posteriori* risk ranking for the various regions becomes that one shown in Fig. 18. Comparing this new ranking with the *a-priori* one of Fig. 15, and assuming the same groupings of regions (with the same colors), it is possible to immediately appreciate two important improvements: (1) the order of the three most damaged northern regions (apart from Lombardia, that is always at the first position) now strictly follows that of both the total cases and deaths in the observed COVID-19 data at April 2, 2020; (2) in the other groups, only the risk of Calabria results to have been overestimated, while only that of Basilicata and Valle d'Aosta have been underestimated (the former for the total cases, the latter for the number of deaths). Also Marche seems to have been quite underestimated, even it is in the right group.

This finding definitely confirms that our model, in both its general and adapted version, is able to distinguish pretty well those that are by far the most damaged regions, all belonging to north of Italy, from those belonging to center and south, as also summarized in Fig. 19. Here, the percentages of damages (cases and deaths) in these three macro-regions at April 2, 2020, are compared with the percentages of cumulated risk associated to the same macro-regions: again, the correlation is evident, for both the *a-priori* and the *a-posteriori* risk indexes, at least at this level of aggregation.

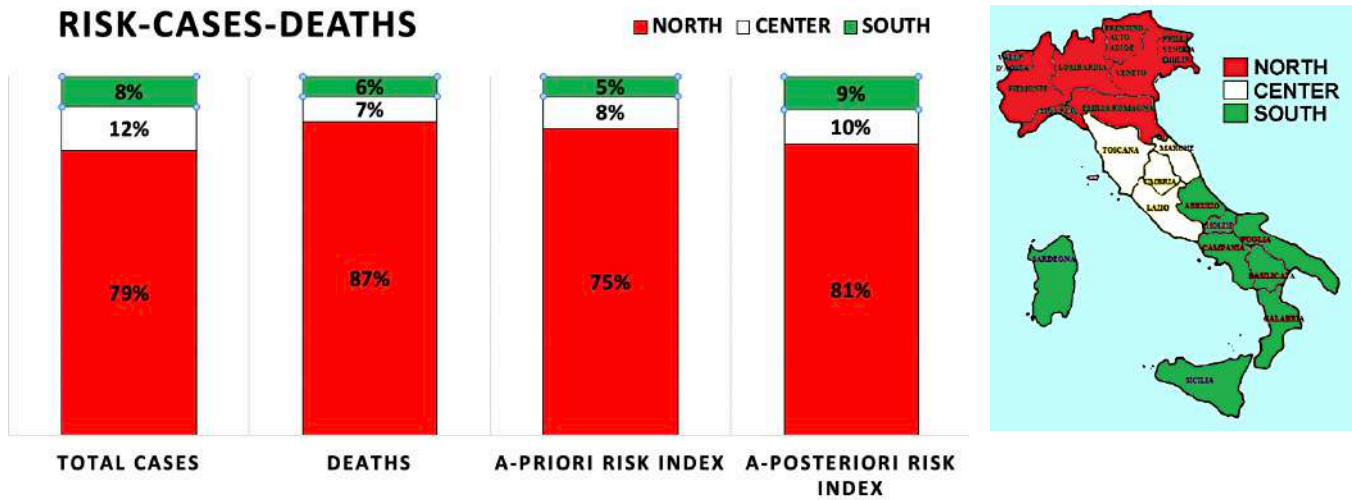


Figure 19: The percentages of COVID-19 total cases and deaths in the three Italian macro-regions (North, Center and South), updated at April 2 2020, are reported together with the corresponding percentages of cumulated risk, both a-priori and a-posteriori. It is clear that our risk indexes are able to explain the anomalous damage discrepancy between these different parts of Italy.

Thus, we can definitely answer to our main question concerning the strong asymmetric distribution of epidemic effects over the Italian territory: it is very likely that it is not a matter of chance; the northern regions are surely the most risky, the most exposed to epidemics like COVID-19 (but not only that), and in principle we could have already known this, since the data about the risk indicators were already available before the COVID-19 outbreak.

Let us now further quantify the correlations of the *a-posteriori* risk ranking of Fig. 18 with the main damage indicators.

In Fig. 20, the same plots than in Fig. 16 are shown, enabling us to appreciate, again, a further improvement with respect to the already very good result obtained with the *a-priori* model. As expected, in almost all the cases, the Pearson coefficients take values higher than before, except for the intensive care occupancy fit performed over all the regions, which maintains the same value (0.98) than in Fig. 16.

Another interesting way to visualize these correlations is to represent the *a-posteriori* risk index through its two main aggregated components, consequences and infection diffusion, and plotting each region as a point of coordinates (I_i, C_i) in the plane $\{I \times C\}$. This kind of Risk Diagram has been reported in Fig.21, where the points have been also characterized by the same color of their group in Fig. 18, indicating a different level of damage (total cases or deaths) observed in the corresponding region at 02/04/2020. Points of regions not correctly identified (because underestimated or overestimated with respect to at least one of the two damage indicators) have been colored in yellow. The position of each point can be compared with a curve that representing the place of the plane points with a risk index equal to the reference value $R_{av} = 0.12$ found for our country (i.e. the average risk for Italy).

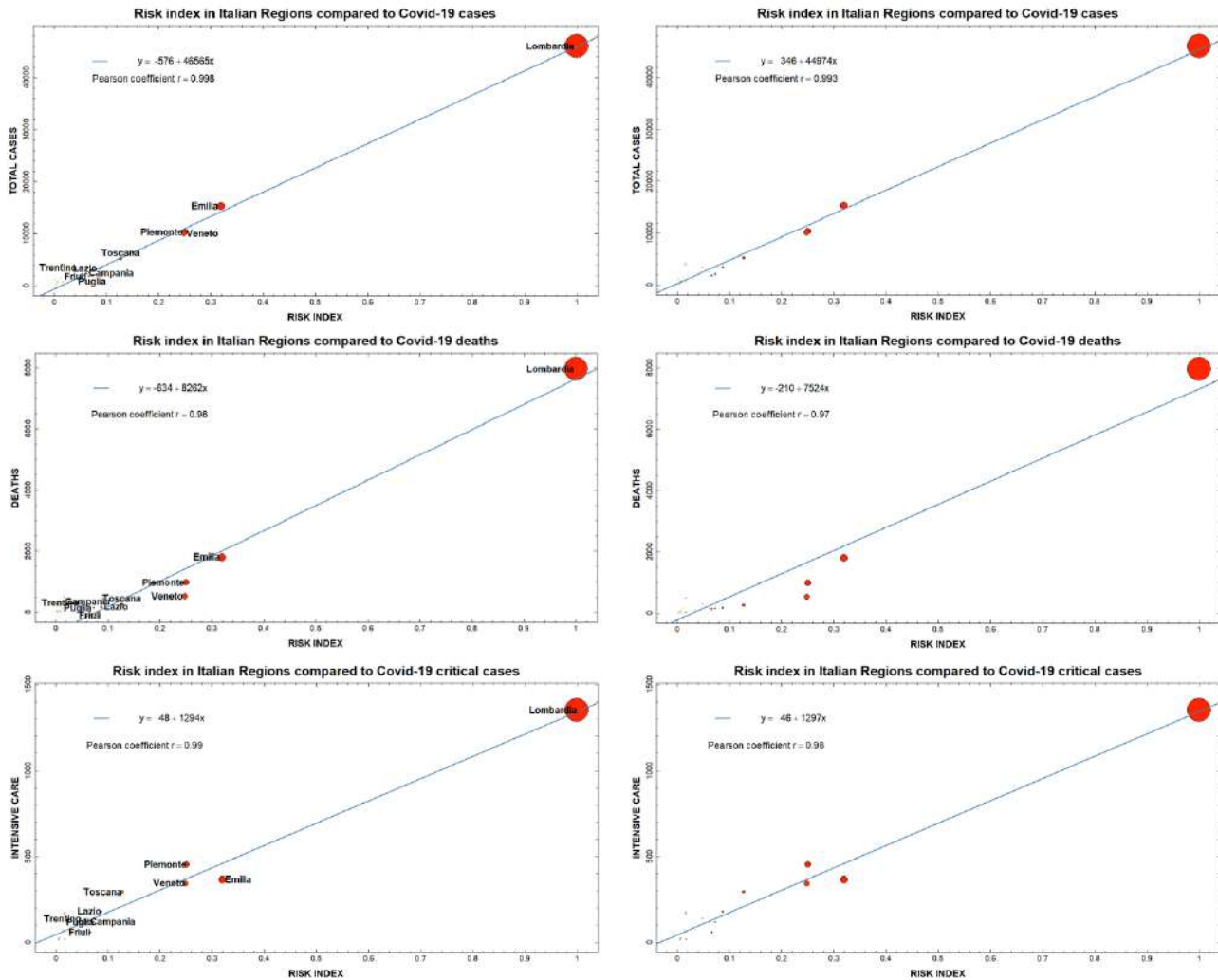


Figure 20: The three main damage indicators (total cases, deaths and intensive care occupancy), updated at April 2 2020, are reported as function of the a-posteriori risk index for all the Italian regions, calibrated on the COVID-19 data. The size of the points is proportional to the risk index score. A linear regression has been performed for each plot, only for the first 10 regions in the ranking (left column) and for all the regions in the ranking (right column). The Pearson correlation coefficients are, in both the cases, very good and higher than the corresponding ones shown in Fig. 16 for the *a-priori* model.

According to equation 8, such a iso-risk curve is a hyperbole, described by the equation $C = R_{av} / I$: all the regions lying above this line have a risk score higher than the average, while all the regions below this line have a risk score lower than the average (the value of the risk index is reported in parentheses next to each region). Again, it clearly appears that our risk analysis is able to correctly identify the four more damaged regions, and also the large majority of the other less damaged regions, with the few exceptions which we have already noticed (i.e. Calabria, Umbria, Valle d'Aosta and, to some extent, also Marche).

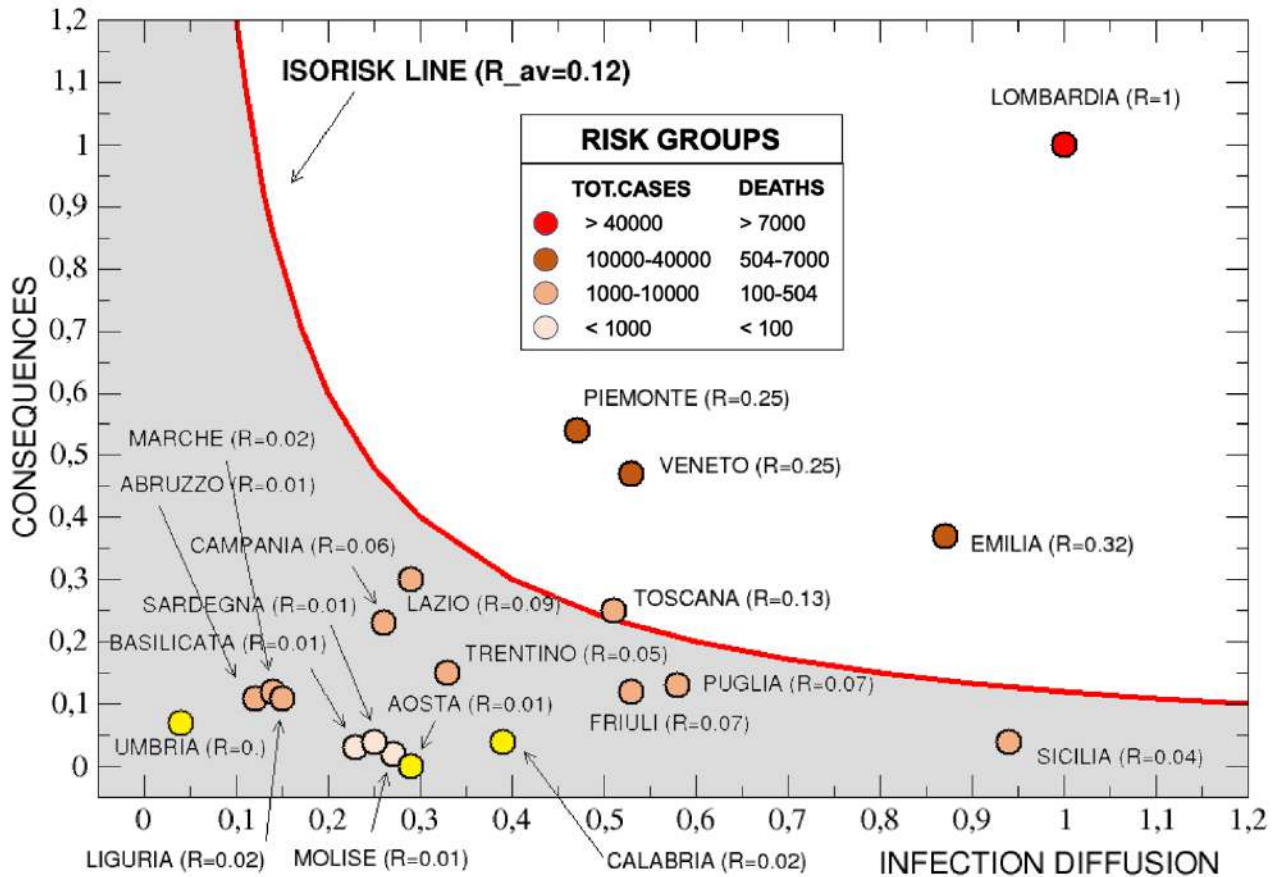


Figure 21: Each region is represented as a point in the plane $\{I \times C\}$ while the color is proportional to the level of damage in that region updated at 02/04/2020. The more damaged regions, in terms of total cases, lie with a good approximation above the $C = R_{av}/I$ hyperbole (i.e. the iso-risk line related to the average regional risk index), while the less damaged ones lie below this line. The *a-posteriori* risk index score is also reported for each region.

In the next section we will see that the methodology we are proposing in this paper, and in particular this kind of representation in terms of risk diagram, could be easily adopted in order, on one hand, to perform an optimization analysis of the *a-priori* risk in terms of potential carrying capacity of the regional health systems and, on the other hand, to extrapolate some policy implications to prevent damages in case of an epidemic outbreak like the COVID-19 one.

Let us close this section by showing, in Fig. 22, three sequences of the geographical distribution of damages (total cases, deaths and intensive care occupancy) as a function of time, from 09/03/20 to 02/04/20, are compared with the geographical map of the *a-priori* risk level (the last image on the right in each sequence), being the latter independent of time. In all the plots, damages seem to spread over the regions with a variable intensity (expressed by the color scale) quite correctly predicted by our risk analysis.

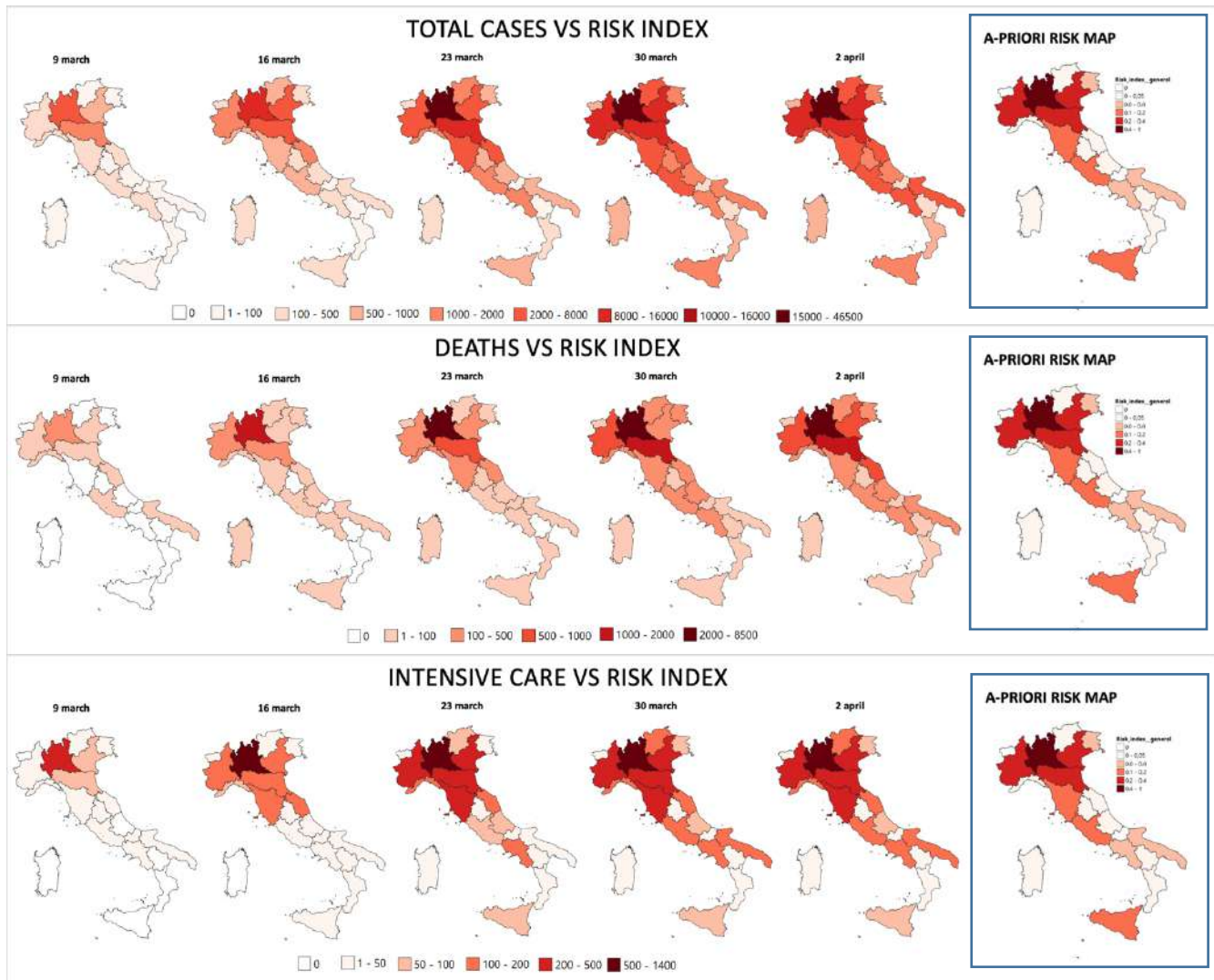


Figure 22: The geographical distribution of several kinds of damages in the various Italian regions is reported as function of time, from 09/03/20 until 02/04/20, and is compared with the geographical distribution of the *a-priori* risk.

5 Policy Implications

Decoupling the risk into two components, one related to the causes of the potential damage (Infection diffusion I) and one concerning the attitude to harm exposed people (Consequences C), might suggest different policy strategies to face the challenges of the epidemics. The first focuses on reducing the causes, i.e. prevention of the infection diffusion, the second relies on reducing the effects on population, i.e. protection. Actually, an optimal mix of the two strategies should be put in place, looking for the maximum output (in terms of consequences reduction) with the least social and economic effort.

In this context, it is evident that enhancing the capability of the healthcare system appears to be the most important action: basically, it is an insufficient carrying capacity that leads to the emergency. This is consistent with what Lombardia has been experimenting in these days. Apart from the factors we identified above as multiplier of the infection spreading, the epidemic crisis of Lombardia seems to be essentially a breakdown of its healthcare system: unusual high demand rate for hospital admissions, long times of intensive therapy required by the virus aggressiveness, insufficient capacity of hospital assistance (diagnosis equipment, staff, spaces, etc.) has led the formation of a “long queue” of sick people, that has exacerbating bad consequences both for lack of medical assistance and probability of more infection spreading.

Data illustrated in the previous section provide a positive analysis of the health system facing an epidemic disease. We now turn to a normative approach in order to present a viable framework to asses possible intervention protocols of policy actions. In particular, several variables affecting the diffusion of an infection can be looked at as policy instruments. The whole set of possible restrictions to the free circulation of people shows, are a valid example. In facing the challenges that the emergency is creating, our simple approach underlines the direction of policies aimed to manage both the spreading process and the stress level to the health-care system of a given district (such as a given country, a region, a urban area, etc.).

5.1 A model of epidemic management

Let $R: (0,1) \times \mathbb{R} \rightarrow \mathbb{R}$ be a C^2 function representing the risk (R) of a community (assumed to be equivalent to that of its policy-maker), determined by two variables, namely the infection ratio ($x \in (0,1)$), intended here as the proportion of infected individuals over the total population, and the impact of consequences caused by the spreading of the disease, measured as the number of per capita hospital beds ($b \in \mathbb{R}$) required by the current situation, i.e., $R = f(x, b)$. It will be assumed, following the view suggested by data and shown above, that both independent variables have a positive but decreasing impact on the level of risk, which is the obvious consequence of the fact that the level of risk is subject to saturation. In Fig. 23, the left panel shows the risk function, while the right panel provides an illustration of the family of its convex contours, for a finite set of risk levels (limited for graphic convenience):

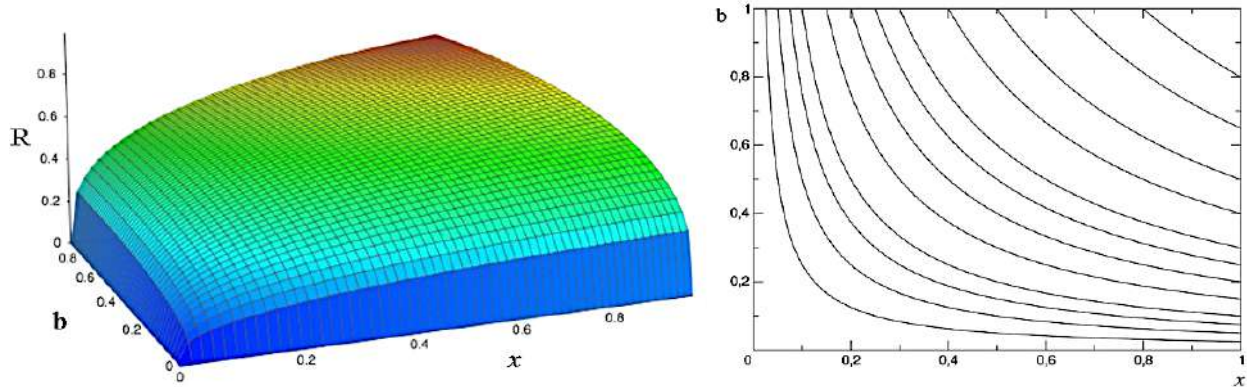


Figure 23: The Risk function and its convex contours: an example for $R = x^{0.5}b^{0.5}$.

As an easy visual comparison shows, the right panel of Fig.23 replicates the meaning of Fig.21 by translating the consequences indicated by data as the required per capita hospital beds while explaining that the position of each iso-risk curve corresponds to the different actual composition of the scenario at hand.

Each community has an exogenously given endowment of hospital beds (H), which can be thought as the structural allowance given by its health-care system. Such a consistence is a dynamic variable that can vary in time. We will proceed with a comparative-static analysis, by presenting a series of intuitions describing possible directions of policy, starting from different initial configurations.

In particular, we model that a part of the global allowance is dedicated to intensive therapy beds, $HH = \alpha H$, $\alpha \in (0,1)$. When the COVID-19 epidemic started its dramatic dynamics, one of the most recurrently investigated aspects was that the available hospital beds in regime of intensive therapy were not enough to cover the potential demand (by then presumed). Indeed, in the absence of a specific pharmaceutical remedy (a specific drug or a vaccine, etc.), the protocol of care for infected people has been defined as an intensive therapy recovery, consisting of auxiliary oxygen provision, deep monitoring and assistance services. Thus, we assume such a unique care strategy in the model and represent the structural carrying capacity of the health care system (Z) as the available number of per capita hospital beds.

The carrying capacity derives from the expenditure in the health care system services G_H , which is set to satisfy, in normal situations, a chosen proportion of the population considered *sufficient*. Such a choice is based on a politic decision and is reasonably inferred from the past experience, by considering structural elements of population, such as the age structure, the density over a given territory, etc. Within the deliberated budget, a proportion is dedicated to set up intensive therapy beds, as an advanced assistance service provision.

It is not surprising that if the context changes because of an emergency, like the one possibly deriving from an epidemic spreading, the number of beds can suddenly reveal insufficient and/or the proportion of intensive therapy beds inadequate.

In our model, the policy maker affects both H and α by G_H , according to the situation at hand. Thus, the carrying capacity is determined as a function of the expenditure and is exploited according to different diffusion ratio of infection. Let $Z : (0,1)^2 \times \mathbb{N} \times \mathbb{R} \rightarrow \mathbb{R}$, be the function representing the carrying capacity, defined as $Z = H - h x n$, where $h = (1 - \alpha)$ and n is the population; in per capita terms, it can be easily rewritten as $z = z_H - hx$, with $z = Z/n$ and $z_H = H/n$. If we restrict the analysis to a comparative statics perspective, as said above, for any given couple (H, α) we can consider a reduced form of the carrying capacity constraint, depending on the infection diffusion rate. In Fig. 23: the left panel shows the carrying capacity of the system, given a pre-determined amount of G_H ; the central panel shows the effects of different changes in the proportion of per capita intensive therapy hospital beds over the total, causing changes in the slope of the line (which becomes steeper for reduction in the proportion of intensive therapy beds); while the right panel shows the effects of changes in the overall expenditure, causing parallel shifts of the line (which is translated above for increments of the expenditure). In particular, it is worth to notice that the assortment of the proportion HH/H may cause that the overall capacity to assist the entire population is not for granted (i.e. the intercept on the x axis might be less than 1).

Simultaneous combination of variations in the total expenditure and in the proportion of intensive therapy beds are of course possible, by giving the actual mix of possibilities that a policy-maker can count on in facing the situation at hand.

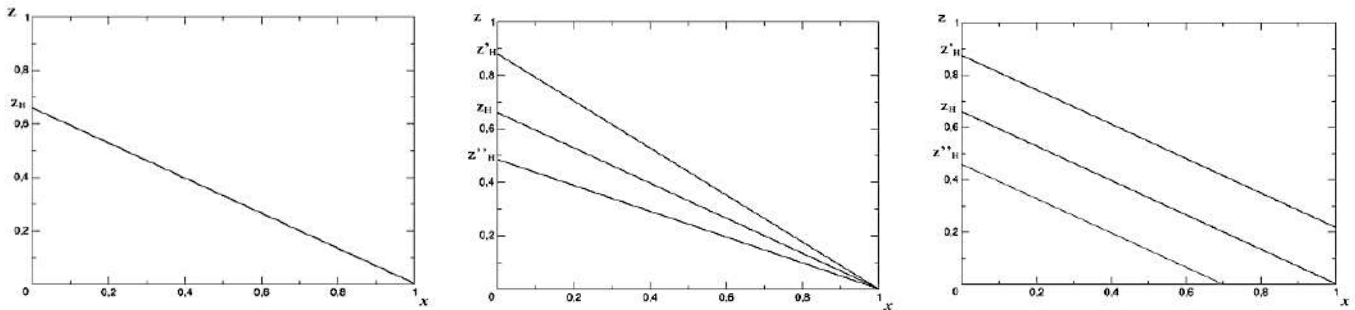


Fig.24: The carrying capacity function and effects of policy interventions on the supply-side

It is natural to imagine that, by definition, an emergency challenges the usual policy settings, since the adjustment speed of actions to new targets may be slower than the speed of damages caused by the emergency itself. A direct comparison of elements contained in Fig. 23 and Fig. 24 provides a quick inspection of the policy problem, focused to control the epidemic spreading.

In the left panel of Fig. 25 such a problem has been depicted by presenting an hypothetic country where a given carrying capacity has to sustain the risk levels represented by different iso-risk curves. Let us hypothesize that the starting point is A, located on the highest curve. Some considerations help explaining the meaning of the model. First of all, without an immediate availability of funds to increase the carrying

capacity, the main policy target could easily be described as the transposition of the iso-risk curve to the bottom-left: the closer the curve to the origin, the higher the satisfaction for the community. Secondly, the meaning of the relationship between the curve and the line is that until the curve touches the line, the policy maker has a sort of measure of how the problem is out of control, as the vertical distance between the curve and the constraint line: indeed, for any infection rate, the required number of per capita hospital beds by the current situation are greater than the available ones. Third, when policies successfully transpose the curve to lower levels (or, equivalently, further expenditure shifts the line upwards), the minimal goal of manageability is reached if both are at least tangent to each other, as depicted in the right panel of Fig.25. Whenever such a tangency condition has been reached, the highest infection rate that the given health care system can sustain has been found. There would still be room for further policy actions, aimed either to approach a lower iso-risk curve or to save resources and/or re-allocate them differently, by modifying the desired combination of infection rate and hospital beds (i.e., a rotation of the constraint to approach a different point along the same iso-risk curve).

When point E is approached, the policy maker knows that the infection ratio that makes the required number of beds equal to the endowment available in the health-care system has been reached. Points F and G, although carrying the same risk level as E, still represent out-of-control positions, for different reasons described below. Both positions would indicate that the policy is still missing the minimally accepted target (i.e., the tangency condition). As shown in the right panel of Fig. 25, a policy that effectively reduced the risk at the level represented by the lowest iso-risk curve, can be considered satisfactory when any of points belonging to the arc TT' is reached, e.g. the point L. Then, the efficacy of performed policy action was able to set part of the carrying capacity free and to reduce the epidemic spreading under control. However, the political debate has to decide when such a reduction is enough or when the iso-risk curve is satisfactorily low. Indeed, it is easy to argue that alternative policies are neither equivalent, nor requiring same actions.

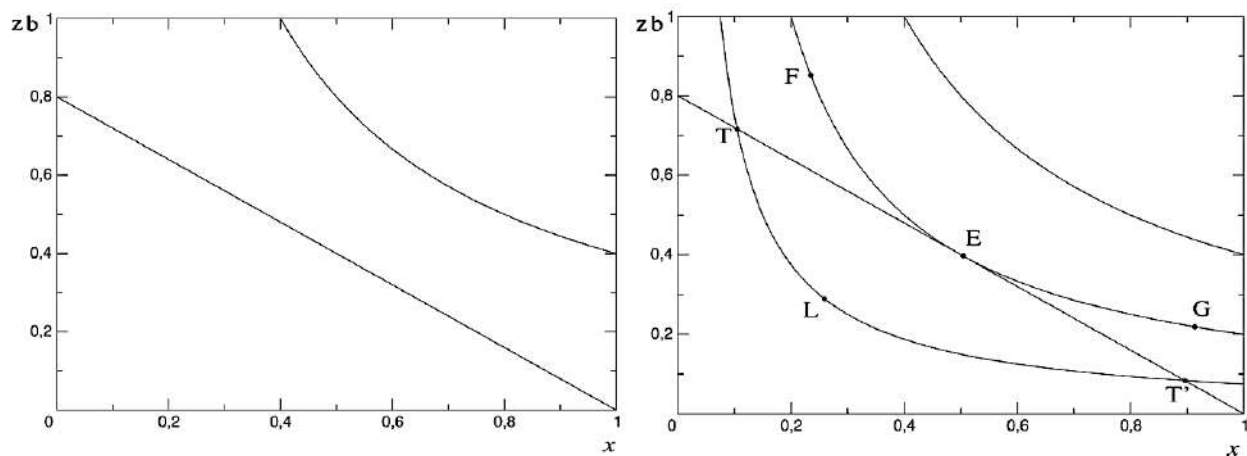


Fig.25: Comparative statics of equilibrium and disequilibrium.

We are aware that the analysis here discussed should be more properly considered within a dynamic model, thus characterizing the rate of utilization of the health-care facilities and the temporal rate of increment of new infections. Nonetheless, as said above, we are restricting our focus here to a simple comparative statics analysis, thus assuming that once that a person enters the health-care system, her place is not available anymore (which is actually true only for a given instant). Despite such a simplification, the model gives a quite intuitive recognition of possible policy directions.

5.2 Policy Intuitions

As said above, the policy problem of an epidemic diffusion can reasonably be defined over a limited scope, basically coincident to a unique target variable, i.e., the resolution of dynamic spreading, such that personal health problems and causalities are under control. Such an essential target can be pursued, in principle, by means of instruments applied to both the supply and the demand side.

It can be useful to look at patients (infected persons) as the demand side looking for health-care services, and to the health-care system as the producer supplying those services.

A basic distinction can be done according to the typology of intervention: demand-side policies are actions devoted to reduce the number of newly infected people; supply-side policies are, instead, aimed to increment the managing capacity of the system.

Examples of demand-side policies are: restrictions to the movement of persons, in general and even for productive reasons; diagnostic activities coupled with dedicated quarantine regulations; prescriptions of precise rules of conduct that effectively fade the contagion out; etc.

Examples of supply-side policies are, instead: expenditure to increase the per capita amount of hospital beds; assortment switching of the ratio of intensive therapy beds relative to total ones; increments in the personnel dedicated to the health-care system; in-house medical care protocols (possibly associated to experimental drugs distribution); etc.

The effects of demand-side interventions are able to move the system over a lower risk contour curve, whereas the effects of supply-side policies are to shift the constraint upwards (and/or change its slope). Both strategies aim to improve the system ability to manage needs of infected citizens.

Consider a couple of examples. First of all, looking at point F and G in the right panel of Fig.22, it is easy to see that both points represent critic situations, requiring different reactions by the policy-maker. In point F, the infection rate is low and, thus, very difficult to be further reduced. Therefore, it is the case to choose a direction towards, for example, health protocols for safe rule of conducts that citizens need to adopt. On the contrary, in point G, the infection rate is so high that strong direction to create a limit on social interaction easily appears to be much more urgent than rules of conduct or medical protocols.

Similar argument can be discussed about which approach (or which mix) between demand-side and supply-side policies is preferable. The evidence that an increment in the expenditure can be more or less effective than a social habit modification is difficult to be found. Just this, alone, could require a very wide political debate. While preserving a basic simplicity, our model has the advantage to provide an intuitive insight on actually complex policy problems deriving from an epidemic emergency.

6 Closing remarks

In this study we have shown that a data-driven epidemic risk analysis performed on the various Italian regions and based on a proper combination of a set of plausible indicators, provides a possible explanation, in terms of a different *a-priori* risk exposure, of the highly asymmetric distribution of damages (in terms of severe cases and deaths) caused by the COVID-19 outbreak, which – at the date of April 2, 2020 – are by far mostly concentrated in the northern Italian regions, resulting relatively harmless in the center and south Italy. Although the first official cases of COVID-19 had been registered already at the end of January 2020 in Lazio, i.e. in a very central and highly connected (in terms of mobility) part of the country, and later on, at the end of February, the first official cases were certified in Lombardia and Veneto, if we consider also the various waves of hundreds of thousand people moving from the northern regions to the central and southern ones before the complete Government lockdown of the country on the 9th of March, we could reasonably think that the virus should have had enough time to almost homogeneously spread all over the Italian regions (at least much more than the official data tell us). On the other hand, the outbreak has not impacted in a homogeneous way in the country. The real mortality data registered at the end of March 2020 show a sudden anomalous peak of deceased cases – likely due to the presence of coronavirus – only in the north but not in the center and south Italy. In addition, COVID-19 epidemic damages are mostly observed in the same regions which saw the highest number of hospitalized and deceased patients also for the seasonal flu epidemic 2019-2020, which had its peak at the end of January 2020. Our analysis shows that this is not a coincidence, since these regions (first of all Lombardia, then Piemonte, Emilia Romagna and Veneto) result to be in the first top positions of our proposed risk ranking, calculated through a combination of three main components (infection diffusion, exposure and vulnerability) directly or indirectly related with a greater probability for a virus to spread and to have a dramatic impact in terms of severe and deceased cases. We believe that, on one hand, the proposed methodology could be further improved with more reliable real data about the current epidemic. In this respect, it would be crucial to test periodically random samples of the population in order to estimate how diffuse the outbreak is at the moment and check in a reliable way its lethality and mortality rates. On the other hand, our analysis could be also very useful to address either *a-priori* or *a-posteriori* policy strategies for preventing or controlling a possible future epidemic, and can be easily adaptable to any geographical zone and at any geographical scale (regional, national, international). In particular, our analysis could be also quite useful in the current phase, in which policy-makers are

considering possible strategies to diminish the lockdown, since it seems to suggest that a good solution for gradually reopening the country could be that of considering first those regions characterized by a lower risk.

Acknowledgments

AEB, AP and AR acknowledge financial support of the national project PRIN 2017WZFTZP *Stochastic forecasting in complex systems*.

References

- Alirol, E., Getaz, L., Stoll, B., Chappuis, F., & Loutan, L. (2011). Urbanisation and infectious diseases in a globalised world. *The Lancet infectious diseases*, 11(2), 131-141.
- Babayev, G., Ismail-Zadeh, A., Le Mouël, J. L., & Contadakis, M. E. (2010). Scenario-based earthquake hazard and risk assessment for Baku (Azerbaijan). *Natural Hazards & Earth System Sciences*, 10(12).
- Bukhari, Q., & Jameel, Y. (2020). Will Coronavirus Pandemic Diminish by Summer?. Available at SSRN 3556998.Sxansk
- Chan, K. H., Peiris, J. S., Lam, S. Y., Poon, L. L. M., Yuen, K. Y., & Seto, W. H. (2011). The effects of temperature and relative humidity on the viability of the SARS coronavirus. *Advances in virology*, 2011.
- Charaudeau, S., Pakdaman, K., & Boëlle, P. Y. (2014). Commuter mobility and the spread of infectious diseases: application to influenza in France. *PloS one*, 9(1).
- Chinazzi M. et al. , 2020, *The effect of travel restrictions on the spread of the 2019 novel coronavirus (COVID-19) outbreak*, Science 10.1126/science.aba9757
- Chowel G. Fuentes R. Tower S. Sotomajor V, 2012. The influence of climatic conditions on the transmission dynamics of the 2009 A/H1N1 influenza pandemic in Chile. *BMC infectious diseases* 12: 298
- Collins, T. W., Grineski, S. E., & Aguilar, M. D. L. R. (2009). Vulnerability to environmental hazards in the Ciudad Juárez (Mexico)–El Paso (USA) metropolis: a model for spatial risk assessment in transnational context. *Applied Geography*, 29(3), 448-461.
- Crichton D. , 1999, *The Risk Triangle*. Natural disaster management: a presentation to commemorate the International Decade for Natural Disaster Reduction(IDNDR), 1990-2000Ingleton J: Tudor Rose; 1999.
- Cui, Y., Zhang, Z. F., Froines, J., Zhao, J., Wang, H., Yu, S. Z., & Detels, R. (2003). Air pollution and case fatality of SARS in the People's Republic of China: an ecologic study. *Environmental Health*, 2(1), 15.

Epicentro 2020, <https://www.epicentro.iss.it/influenza/flunews#casi>

Fanelli D. , Piazza F., 2020, *Analysis and forecast of COVID-19 spreading in China, Italy and France*, arXiv:2003.06031

Flaxman S. et al. 2020, *Estimating the number of infections and the impact of non- pharmaceutical interventions on COVID-19 in 11 European countries*, <https://www.imperial.ac.uk/media/imperial-college/medicine/sph/ide/gida-fellowships/Imperial-College-COVID19-Europe-estimates-and-NPI-impact-30-03-2020.pdf>

Giovanetti M., Angeletti S. , Benvenuto D., Ciccozzi M., 2020, *A doubt of multiple introduction of SARS-CoV-2 in Italy: A preliminary overview*. *J Med Virol*. Mar 19. doi: 10.1002/jmv.25773.

GitHub Repository COVID-19 2020, <https://github.com/pcm-dpc/COVID-19>

Hoffmann et al. , 2020, *SARS-COV-2 cells entry depends on ACE2 and TMPORSS2 and is blocked by a clinically proven protease inhibitor*, *Cell* 181, 1–10 April 16, 2020 a 2020 Elsevier Inc.

IPCC, C. C. (2014). *Synthesis Report, Contribution of Working Groups I, II and III to the Fifth Assessment Report of the Intergovernmental Panel on Climate Change, 2014*, IPCC, Geneva, Switzerland..

ISFORT. (2019). 16° Rapporto sulla mobilità degli italiani. www.isfort.it

Italian Department for Economic Policy Planning and Coordination, <http://www.urbanindex.it/>

Kim, H., Park, J., Yoo, J., & Kim, T. W. (2015). *Assessment of drought hazard, vulnerability, and risk: A case study for administrative districts in South Korea*. *Journal of Hydro-environment Research*, 9(1), 28-35.

Kron W., 2002, *Flood risk = hazard x exposure x vulnerability*. In: Wu M. et al., (ed.), *Flood Defence*, Science Press, New York, 82-97.

Magdon-Ismail M., 2020, *Machine Learning the Phenomenology of COVID-19 From Early Infection Dynamics*, medRxiv preprint doi: <https://doi.org/10.1101/2020.03.17.20037309>.

Makinen TM., Juvonen R., Jokelainen J., Harju HT., Peitso A., Bloigu A., Kassinen SS., Leinonen M., Hassi J. (2009) *Cold temperature and low humidity are associated with increased occurrence of respiratory tract infections*. *Respiratory Medicine* 103: 456-462.

Miller A., Reandelar M.J., Fasciglione K., Roumenova V., Li Y., and Otazu G.H., 2020, *Correlation between universal BCG vaccination policy and reduced morbidity and mortality for COVID-19: an epidemiological study*, medRxiv preprint doi: <https://doi.org/10.1101/2020.03.24.20042937>.

MS 2020, *Report of the Italian Health Ministry on daily mortality surveillance, 2020 in Italian* http://www.epiprev.it/sites/default/files/SISMG_COVID19_28032020.pdf

Peiris JS, Yuen KY, Osterhaus AD, Stöhr K 2003. *The severe acute respiratory syndrome*. N Engl J Med.;349(25):2431-41. <https://doi.org/10.1056/NEJMra032498> PMID: 14681510

Pepe E., Bajardi P., Gauvin L., Privitera F., Cattuto C., Tizzoni M., 2020, *COVID-19 outbreak response: first assessment of mobility changes in Italy following lockdown*, COVID-19 Mobility Monitoring project

Pinotti F., Di Domenico L., Ortega E., Mancastroppa M., Pullano G., Valdano E., Boëlle P-Y., Poletto C., Colizza V., 2020, “*Lessons learnt from 288 COVID-19 international cases: importations over time, effect of interventions, underdetection of imported cases*” , medRxiv preprint doi <https://doi.org/10.1101/2020.02.24.20027326>.

Setti L. et al. , 2020, Position paper: *Relazione circa l'effetto dell'inquinamento da particolato atmosferico e la diffusione di virus nella popolazione* , SIMA

Stein, R. A. (2011). Super-spreaders in infectious diseases. International Journal of Infectious Diseases, 15(8), e510-e513.

Stier A., Berman M.G., Bettencourt L.M.A., 2020, *COVID-19 attack rate increases with city size*, arXiv:2003.10376

Thomalla, F., Downing, T., Spanger-Siegfried, E., Han, G., & Rockström, J. (2006). Reducing hazard vulnerability: towards a common approach between disaster risk reduction and climate adaptation. Disasters, 30(1), 39-48.

Tomlinson, C. J., Chapman, L., Thornes, J. E., & Baker, C. J. (2011). Including the urban heat island in spatial heat health risk assessment strategies: a case study for Birmingham, UK. International journal of health geographics, 10(1), 42. GitHub Data Set gives updated data coming from Italian Health Ministry: <https://github.com/pcm-dpc/COVID-19>

Villa M. *ISPI report 2020*, <https://www.ispionline.it/it/pubblicazione/coronavirus-la-letalita-italia-tra-apparenza-e-realta-25563>

Worldometer 2020 - see the link https://www.worldometers.info/world-population/population-by-country/?fbclid=IwAR1IDyHcHKefHTuxw_T57IqirmcvMKIsUiiLRE1BHMciX0K2GxfJaRK8f2M

Zhang Y-Z. , 2020, *Novel 2019 coronavirus genome*. Virological. Available from: <http://virological.org/t/novel-2019-coronavirus-genome/319>